Subcellular Biochemistry 71

E. Anibal Disalvo *Editor*

Membrane Hydration

The Role of Water in the Structure and Function of Biological Membranes

Springer

Subcellular Biochemistry

Volume 71

Series Editor
J. Robin Harris
University of Mainz, Mainz, Germany

The book series SUBCELLULAR BIOCHEMISTRY is a renowned and well recognized forum for disseminating advances of emerging topics in Cell Biology and related subjects. All volumes are edited by established scientists and the individual chapters are written by experts on the relevant topic. The individual chapters of each volume are fully citable and indexed in Medline/Pubmed to ensure maximum visibility of the work.

More information about this series at http://www.springer.com/series/6515

E. Anibal Disalvo
Editor

Membrane Hydration

The Role of Water in the Structure and Function of Biological Membranes

Springer

Editor
E. Anibal Disalvo
Laboratorio de Biointerfases y Sistemas Biomimeticos
Centro de Investigacion y Transferencia de Santiago del Estero
Universidad Nacional de Santiago del Estero-Consejo Nacional de Investigaciones Científicas y Técnicas
Santiago del Estero, Argentina

ISSN 0306-0225
Subcellular Biochemistry
ISBN 978-3-319-19059-4 ISBN 978-3-319-19060-0 (eBook)
DOI 10.1007/978-3-319-19060-0

Library of Congress Control Number: 2015951200

Springer Cham Heidelberg New York Dordrecht London

Printed on acid-free paper

Springer International Publishing AG Switzerland is part of Springer Science+Business Media (www.springer.com)


SANTIAGO DEL
ESTERO,
ARGENTINA

stn@cmu.edu

Water, water, everywhere,
And all the boards did shrink;
Water, water, everywhere,
Nor any drop to drink.

The Rime of the Ancient Mariner
Samuel Taylor Coleridge (1797)

stn@cmu.edu

Preface

Biological membranes are unique material in terms of surface and mechanical properties due to its contact with water, and nowadays important attempts to mimic their properties in the search of biotechnological inputs in human health, food industry, crop, and energy have been developed. Thus, hydration in membranes gets new insights from the prospect of nanosystems.

Hydration is an emerging subject in the field of material sciences. In particular, in biological systems water is organized in proteins and membranes. In this last case, the amount of water average is no more than 20–25 molecules per lipid. If it is considered that it may be distributed in discrete sites of different chemical features, water environments are restricted to less than ten water molecules. With this criterion, studies of water in biological systems in general, and in membranes in particular, are within the scope of nanosciences.

This book is an effort to enlighten the importance of this subject in relation to biology and biophysics. This project has been possible due to the enthusiasm of all the authors of the chapters to which I want to particularly thank for their work.

I also like to recognize those who for different reasons could not contribute to this edition and hope that they may enrich future ones.

Among the authors I am particularly grateful to Zoran Arsov, Stephanie Tristram-Nagle, Helge Pfeiffer, and Gustavo Appignanessi for their help, advice, and comments along the preparation of the manuscripts.

The ideas about membranes and water have been built along years, and therefore, it is the product of what I have been able to collect from excellent teachers, colleagues, and friends.

For this reason I want to specially express my gratitude and recognition to Dr. Jorge Arvia and Dr. Hector Videla from INIFTA (Universidad Nacional de La Plata) with whom I began my feeling for research in biophysical chemistry and bioelectrochemistry during my PhD thesis, to Prof Raul Grigera who showed me the importance of water, and to Prof Hans de Gier from Utrecht University who introduced me in the world of lipids as a postdoc.

Also, I learned thermodynamics with Ernesto Timmermann and lipid monolayers with Bruno Maggio. With all of them I had exciting and vigorous discussions.

A special place is reserved for Sid Simon and Tom McIntosh with whom I spend my sabbatical enjoying science, tennis, and drinks.

Finally I want also to thank all the students who went through my laboratory in the Universidad Nacional de La Plata, University of Buenos Aires, University of Tucuman, and, in these last years, the University of Santiago del Estero, because along their works, their doubts, their achievements, their challenges, and their irreverences I, found new routes to pursue in this research.

I hope that this book will encourage them and the next ones in the fascinating field of biophysics of biological membranes.

Santiago del Estero, Argentina E. Anibal Disalvo

Acknowledgments

The editor is grateful to

Prof. Gerardo Fidelio (Universidad Nacional de Cordoba),
Prof Laura Bakas (Universidad Nacional de La Plata),
Dr. Maria de los Angeles Frías (CITSE, Universidad Nacional de Santiago del Estero-CONICET (RA)), and
Prof. Daniel Rodrigues (Universidad Nacional del Litoral)

for their contributions in the revision of the chapters.

E. Anibal Disalvo
(Editor)

stn@cmu.edu

Contents

Contributors

S.A. Accordino Departamento de Química and INQUISUR-UNS-CONICET, Universidad Nacional del Sur, Bahía Blanca, Argentina

Laureano M. Alarcón Departamento de Química and INQUISUR-UNS-CONICET, Universidad Nacional del Sur, Bahía Blanca, Argentina

Gustavo A. Appignanesi Departamento de Química and INQUISUR-UNS-CONICET, Universidad Nacional del Sur, Bahía Blanca, Argentina

Zoran Arsov Laboratory of Biophysics, Department of Solid State Physics,"Jozef Stefan" Institute, Ljubljana, Slovenia

Luis A. Bagatolli Membrane Biophysics and Biophotonics Group/MEMPHYS-Center for Biomembrane Physics, Department of Biochemistry and Molecular Biology, University of Southern Denmark, Odense M, Denmark

John H. Crowe Department of Molecular and Cellular Biology, University of California, Davis, CA, USA

Srinivasan Damodaran Department of Food Science, University of Wisconsin-Madison, Madison, WI, USA

E. Anibal Disalvo Laboratorio de Biointerfases y Sistemas Biomimeticos, Centro de Investigacion y Transferencia de Santiago del Estero, Universidad Nacional de Santiago del Estero-Consejo Nacional de Investigaciones Científicas y Técnicas, Santiago del Estero, Argentina

Axel Hollmann Laboratorio de Biointerfases y Sistemas Biomimeticos, Centro de Investigacion y Transferencia de Santiago del Estero, Universidad Nacional de Santiago del Estero-Consejo Nacional de Investigaciones Científicas y Técnicas, Santiago del Estero, Argentina

John Katsaras Biology & Soft Matter and Biosciences Division, Oak Ridge National Laboratory, Oak Ridge, TN, USA

Zoltan Kovacs Biomeasurement Technology Laboratory, Kobe University, Kobe, Japan

Department of Physics and Control, Corvinus University of Budapest, Budapest, Hungary

Yosuke Kubota Biomeasurement Technology Laboratory, Kobe University, Kobe, Japan

M. Florencia Martini Instituto de Química y Metabolismo del Fármaco, IQUIMEFA UBA-CONICET, Facultad de Farmacia y Bioquímica, Universidad de Buenos Aires, Buenos Aires, Argentina

J.M. Montes de Oca Departamento de Química and INQUISUR-UNS-CONICET, Universidad Nacional del Sur, Bahía Blanca, Argentina

Marcela A. Morini Departamento de Química and INQUISUR-UNS-CONICET, Universidad Nacional del Sur, Bahía Blanca, Argentina

Jonathan D. Nickels Joint Institute for Neutron Sciences, Oak Ridge National Laboratory, Oak Ridge, TN, USA

Department of Physics, University of Tennessee, Knoxville, Knoxville, TN, USA

Viviana I. Pedroni Departamento de Química and INQUISUR-UNS-CONICET, Universidad Nacional del Sur, Bahía Blanca, Argentina

Helge Pfeiffer Department of Metallurgy and Materials Engineering (MTM), University of Leuven (KU Leuven), Leuven, Belgium

J.A. Rodríguez Fris Departamento de Química and INQUISUR-UNS-CONICET, Universidad Nacional del Sur, Bahía Blanca, Argentina

M. Belén Sierra Departamento de Química and INQUISUR-UNS-CONICET, Universidad Nacional del Sur, Bahía Blanca, Argentina

Stephanie Tristram-Nagle Biological Physics Group, Physics Department, Carnegie Mellon University, Pittsburgh, PA, USA

Roumiana Tsenkova Biomeasurement Technology Laboratory, Kobe University, Kobe, Japan

Abbreviations

$\|F(q_z)\|$	Form factor
18:0:22:5PC	Stearoyldocosapentaenoyl-phosphatidylcholine
18:0-22:6PC	Stearoyldocosahexaenoylphosphatidylcholine
$2D_C$	Hydrocarbon thickness
AFM	Atomic force microscopy
A_L	Area/lipid
B	Bulk modulus
D, D-space	X-ray lamellar D-spacing
d, d-space	X-ray wide-angle chain spacing
D_B	Bilayer thickness
D_H'	Headgroup thickness
DHPC	Dihexadecanoyl-phosphatidylcholine
diC22:1PC	Dierucoylphosphatidylcholine
diphytanoylPC	Diphytanoyl-phosphatidylcholine
DLPC	Dilauroylphosphatidylcholine
DLPE	Dilauroylphosphatidylethanolamine
DLPG	Dilauroylphosphatidylglycerol
DMPC	Dimyristoylphosphatidylcholine
DMPE	Dimyristoylphosphatidylethanolamine
DMPG	Dimyristoylphosphatidylglycerol
DMPS	Dimyristoylphosphatidylserine
DOPC	Dioleoylphosphatidylcholine
DOPG	Dioleoylphosphatidylglycerol
DOPS	Dioleoylphosphatidylserine
DPhPC	Diphytanoylphosphatidylcholine
DPPC	Dipalmitoylphosphatidylcholine
DSC	Differential scanning calorimetry
DSPC	Distearoylphosphatidylcholine
EggPC	Egg phosphatidylcholine
EPR	Electron spin resonance
FTIR	Fourier transform infrared resonance

$I(q_z)$	X-ray intensity
interdig.	Interdigitated
K_C	Bending modulus
MD simulation	Molecular dynamics simulation
MLVs	Multilamellar vesicles
NIR	Near-infrared
NMR	Nuclear magnetic resonance
n_W	Number of waters/lipid
n_W'	Steric number of waters/lipid
OSM	Osmotic stress method
PCA	Principal component analysis
PLS	Partial least squares
POPC	Palmitoyloleoylphosphatidylcholine
POPG	Palmitoyloleoylphosphatidylglycerol
PPM	Piezotropic phase transitions method
PrP	Prion protein
SFA	Surface force apparatus
SIMCA	Soft independent modeling of class analogy
SOPC	Stearoyloleoyl-phosphatidylcholine
SOPG	Stearoyloleoylphosphatidylglycerol
Tm	Main transition melting temperature
TMCL	Tetramyristoylcardiolipin
TPM	Thermotropic phase transition method
ULVs	Unilamellar vesicles
u_n	Vertical displacement
V_L	Molecular volume/lipid
V_W	Molecular volume/water
WAMACS	Water matrix coordinates
WASP	Water spectral pattern
η	Fluctuation parameter

Chapter 1
Membrane Hydration: A Hint to a New Model for Biomembranes

E. Anibal Disalvo

Abstract The classical view of a biological membrane is based on the Singer-Nicholson mosaic fluid model in which the lipid bilayer is the structural backbone. Under this paradigm, many studies of biological processes such as, permeability, active transport, enzyme activity and adhesion and fusion processes have been rationalized considering the lipid membrane as a low dielectric slab of hydrocarbon chains with polar head groups exposed to water at each side in which oil/water partition prevails. In spite of several analyses and evidence available in relation to membrane hydration, water is not taken into account as a functional component. For this purpose, new insights in the water organization in restricted environments and the thermodynamical and mechanical properties emerging from them are specifically analysed and correlated.

This chapter summarizes the progress of the studies of water in membranes along the book in order to give a more realistic structural and dynamical picture accounting for the membrane functional properties.

Keywords Water penetration • Interphases • Hydration water • Confined water • Complex systems • Membrane models

1.1 Introduction

Cell membranes are the physical limit between the living and the non-living world. If the interior of the cell is considered the actual place of reproduction, compartmentalization gives the appropriate environment to biological metabolic reactions and the highly selective kinetic barrier properties of the membrane regulate the exchange of matter and energy with the surroundings (Yeagle 2004).

Biomembranes are self organized assemblies of lipids and proteins, The classical view of a biological membrane is based on the Singer-Nicholson mosaic fluid model

E.A. Disalvo (✉)
Laboratorio de Biointerfases y Sistemas Biomimeticos, Centro de Investigacion y Transferencia de Santiago del Estero, Universidad Nacional de Santiago del Estero-Consejo Nacional de Investigaciones Científicas y Técnicas, 4200 Santiago del Estero, Argentina
e-mail: disalvoanibal@yahoo.com.ar

E.A. Disalvo (ed.), *Membrane Hydration*, Subcellular Biochemistry 71,
DOI 10.1007/978-3-319-19060-0_1

in which the lipid bilayer is the structural backbone (Singer and Nicolson 1972). In this context, the lipid membrane was usually described by a low dielectric slab of hydrocarbon chains with polar head groups exposed to water at each side in which oil/water partition prevailed (Overton 1889; Al-Awqati 1999).

Many studies of biological processes such as, permeability, active transport of ions, enzyme activity and adhesion and fusion have been rationalized under this paradigmatic model of sticks and balls in which different proteinaceous particles were inserted to explain biological activity that the single non polar slab could not explain.

In the last years, several critical reviews have introduced changes in the proposal of Singer and Nicholson by including lipid mixtures, lipid heterogeneities, rafts, local curvatures and protein-lipid interactions (Israelachvili 1977; Ti Tien and Ottova 2001; Bagatolli et al. 2010; Goñi 2014). However, in spite of several analyses and evidence available in relation to membrane hydration (Jendrasiak and Hasty 1974; Jendradiak et al. 1996; Israelachvili and Wennerström 1996) the principal feature of the classical view still remained: water is not taken into account as a functional component. To put emphasis in the importance of the structural/thermodynamic properties of water relevant to membrane response, a thorough revision is imperative.

As said elsewhere, water has been for biologists as the canvas for the painters. All is stabilized by water but consideration of water incorporated in the final structure and the dynamical (thermodynamic and mechanical) properties it imposes to the ensemble is far from being a routine.

As pointed out by Damodaran in Chap. 10, "although it is well recognized that structural evolution of proteins and formation of lipid vesicles and cell membranes are simple manifestations of the hydrophobic effect, i.e., a consequence of energetics of interaction of water with the apolar moieties of these molecules, the possibility of water playing a vital role in the very functioning of these biological systems is often overlooked".

Moreover, a non-negligible number of works deals with biological mechanisms as they would occur in an anhydrous state or ignoring water in structure and kinetics processes.

This book is an attempt to organize in a rationale way the progress of the studies of water in membranes that give place to different biological phenomena.

For this purpose, new insights in the water organization in restricted environments and the thermodynamical and mechanical properties emerging from them are specifically analysed and correlated, in order to give a more realistic structural and dynamical picture accounting for the biological functional properties.

The main points that deserve special attention are:

- water penetration and distribution along the lipid molecules
- water mediation in the interaction between lipid membranes (adhesion, fusion) or a lipid membrane and a protein (lipid-protein interaction) through water structure (hydration force, hydration layers)
- surface pressure and its implications in surface water activity.
- water mediation in enzyme activity

1.2 Water Penetration and Distribution Along the Lipid Molecules

In terms of Tristram-Nagle (Chap. 2); "why should we be concerned about the number of waters per lipid?". The reason given is that if lipids become too dehydrated, their physical and structural properties change.

Lipid membranes are not formed in the absence of water. With this premise, life is not possible without water (Crowe, Chap. 11). This view justifies the role of water for the thermodynamic stability and assembly of lipids in membranes. However, this is just a beginning and there are several additional points to consider in terms of the bilayer as a complex material system. Some compounds may stabilize biological structures in the absence of water mimicking its hydrogen bonding patterns (Chap. 11). However, for a biological system to work (grow and reproduce) water as a liquid should be present. Thus, the peculiar physical chemical properties of water as a liquid should be considered (Chaplin 1999).

In the seventies, some results in permeability gave place to think about an active role of water in membrane processes although in a naïve and indirect way. Permeation of polar solutes through lipid bilayers, such as glycerol and erythritol among others, was explained by the rupture of H bonds of the solute with the water phase before partitioning into the membrane. These papers (de Gier et al. 1971; McElhaney et al. 1973) explained the process considering that the lipid membrane was composed by a hydrocarbon phase in which only non polar solutes could dissolve. However, at this point no consideration of the role of water in the membrane structure was done, i.e. the permeability barrier of the lipid membrane was imagined as a low dielectric slab, based on Overton rule (Overton 1889; White 1976) which rejected polar and charged compounds and readily dissolved non polar solutes. That is why the authors proposed a dehydration and a particular conformation of the permeant polyols to explain partitioning into the non polar phase.

Further analysis of the permeation of erythritol and glycerol (Disalvo and de Gier 1983) demonstrated that the thickness of the lipid barrier was not only composed of the bimolecular lipid leaflet but, also of a slab of 10 Å thick at each side due to non-solvent water. Equilibrium dialysis experiments used to measure excluded volumes for the non-electrolyte permeant [U-^{14}C] erythritol in lipid bilayer systems indicated a measurable amount of water associated with the lipid membrane similar to that found by calorimetric measurements (22–24 water molecules per lipid in liquid crystalline membranes of phosphatidylcholine) (Chapmann 1971; Chapmann et al. 1974).

Further studies located this region, named as the interphase, between two ideal planes: one at the carbonyl level that defines the interface between the hydrocarbon region and the polar head group region and the other at the external plane along the hydrated phosphates of the phospholipids (McIntosh et al. 1989).

The membrane system was then described as a composite element consisting of the lipid bilayer and adjacent water layers on both sides from which permeant is excluded showing that the water layers contribute to the permeability barrier.

The notion of excluded volume of lipids and water for solutes, implied that membrane matrix was able to offer empty spaces into which molecules of different sizes were able to insert in order to cross it. Although in principle this was treated in terms of geometry, the thermodynamic counterpart was appearing. In this regard, analysis of the permeation of non electrolytes showed that permeability activation energies were consistent with the hydration state of the liposomes. When liposomes were previously shrunken in a hypertonic medium, the activation energy value was considerably lower in comparison with that obtained when liposomes were maintained in an isotonic state (Disalvo 1986 and references therein). This indicated that the main barrier for permeation kinetics was affected by the water/lipid ratio n_W.

The inclusion of water in the lipid bilayer does not only affect the thickness, influencing the permeability coefficient derived from the first Fick law, but also the phase transition temperature. As pointed out in Chap. 2, when the hydration level in phosphatidylcholines drops below 20 wt.% water ($n_W = 12$), the measured T_m (main chain melting) increased dramatically.

In addition to thickness, increase in n_W generally increases the area per lipid, another parameter affecting permeability, both in the gel and fluid phases. Small Angle X-Ray Scattering (SAXS) indicated that the phase transition of lipid membranes leads to a membrane thickness decrease and an area per lipid increase (Ipsen et al. 1990). Concomitantly, in this condition, the increase in the trans-gauche isomers in the lipid acyl chains produces a higher disorder state identified as "kinks", where water molecules can fit (Träuble 1971).

The larger lipid areas require more water, according to Tristram-Nagle (Chap. 2). On the other way round, water exchange between lipids in the membrane and the bulk can occur with changes in the area per lipid. This point is essential to the approach developed in Chaps. 9 and 10 where changes in monolayer surface pressures are discussed in terms of water activity.

The headgroup structural water, shown in Fig. 2.7 of Chap. 2, is considered to be a lower limit to measurements of tightly bound water. This water includes the first six water molecules bound to the phosphate and additional six in carbonyl groups (Goñi and Arrondo 1986; Disalvo et al. 2008; Nagle and Tristram-Nagle 2000). Nowadays, water beyond this limit appears to play a role in the process of several peptide and amino acid insertion and enzymatic reactions (Chaps. 9 and 10).

The interpretation of the permeability processes described above maintained the paradigm that the bilayer was totally impermeable to water. But this could not be sustained longer after the finding of Van Zoelen et al. (1976) based on the Kedem and Katchalsky Thermodynamic of Irreversible Process (TIP) formalism. Kedem and Katchalsky (1958) demonstrated the simultaneous non-independent permeation of non-electrolytes and water, i.e. water permeation affects the permeation of the non-electrolytes and vice versa. According to de Gier (1989), the exchange of water molecules across the membrane under equilibrium conditions is disturbed by the solute, producing a net additional flux of water molecules coupled with it. This assumes that non-electrolyte is acting as a carrier or inducing an additional flow of water into the membrane. In thermodynamic language, this can be rephrased by saying that the diffusion of the non electrolyte into the membrane phase produces

a change in the water activity driving a water flux to compensate it. This can be explained considering a chemical equilibrium when lipids are dispersed in an excess of water. Membrane structure is stabilized with a given amount of water forming part of its structure. When a solute enters the lipid matrix, probably dissolving in water between the acyl chains occupying the kinks, a difference in the chemical potential of water is produced and a water influx occurs to reach again the equilibrium. This process is similar to osmosis and the swelling of the membrane matrix may produce water paths expanding the membrane. This is congruent with the leak of ions contained in the liposome interior during hypotonic swelling. These arguments not only introduce water as a structural component in the membrane phase but as an unavoidable element in the thermodynamic response.

The formalism of Thermodynamics of Irreversible processes (TIP) denotes that water not only associates with lipid head groups (Griffith et al. 1974), but also with many of the other membrane's functional groups – in addition to occupying free volume – and considers the possibility that water may be found also in the hydrocarbon region in a limited amount. According to Träuble (1971) and Haines and Liebovitch (1995) the movement of water molecules across membranes can be produced as a consequence of the thermal fluctuations of the conformational isomers in the hydrocarbon chains of the membrane lipids resulting in the formation of so-called "kinks" (Trauble 1971 and, Flory 1969).

Details of the correlation between chain conformation and water states have been published recently (Disalvo et al. 2013).

The need to introduce the interphase region in a model to account many of the molecular details regarding ions, lipids, and more importantly, the solvent permeation is anticipated by Nickels and Katsaras in Chap. 3. The order parameter defined by the geometrical and dynamical restrictions imposed to water molecules by the bilayer, bring the presence of hydrogen bond partners, hydrogen bond lifetimes, and dynamical retardation factors that are analysed later on Chap. 7 by Alarcon et al.

According to Nickels and Katsaras, the rate controlling step is the head group region, which is being modulated by the area of the lipid head group relative to the area per lipid (Mathai et al. 2008). This important insight arises from a deep structural understanding of lipid hydration mentioned in this chapter. From those studies, it is clear that the area per lipid scales with the number of water molecules associated with the head group region. It is natural then, to take into account this information to model water permittivity following an improved criterion of the solubility-diffusion but considering a more complex structure than that corresponding to a single non polar slab as previously considered.

In this regard it is worthwhile to recall that some permeation processes has been interpreted with an approach considering pore formation in contraposition to the solubility/diffusion one. This approach describes water transport considering the line tension, γ, which stabilizes the bilayer, and the surface tension, Γ, which stabilizes a pore of radius r. These quantities, line tension and surface tension as parameters relating to bilayer stability, imply that pores appear more frequently in unstable bilayers. The classical view of a pore comes from the idea that water

molecules pave paths across the membrane as a stationary phase and mobile waters displace as in bulk water in the center of the pore. This view can only be sustained assuming large amounts of water in the pore. The radius of the pore is in terms of number of water molecules of only two to four water molecules. The meaning in this context of instability is a matter of discussion that is analyzed by Bagatolli (Chap. 5), Disalvo (Chap. 9) and Damodaran (Chap. 10).

1.3 Water in Membrane Structure and the Interfacial Properties

To relate surface tension and contraction/expansion phenomena exclusively to pore formation is questionable. A rigorous analysis of the thermodynamics of lipid monolayers and bilayers demonstrates that solubility/diffusion criterion also involves membrane area and surface pressure changes (Chaps. 9 and 10), which shows that classical partition of solutes is not correct in lipid phases constituted by a two molecular thick layer apposed to each other by the hydrocarbon chains. Moreover, the heterogeneous distribution of water in the lipid matrix in which different water species, in terms of the number and type of hydrogen bonds of water molecules between them and with the lipid residues, can be found, is against the notion of partition in a single hydrocarbon slab.

The expansion of the membrane by water penetration involves other properties of the lipid membrane. In this regard, the chapter by Pfeiffer (Chap. 4) brings about several important considerations of lipid membranes as a unique material.

In this Chapter, an overview on the theory of hydration forces, ranging from polarisation theory to protrusion forces, based on a selection of appropriate experimental techniques, such as X-ray diffraction, atomic force microscopy and calorimetry, is presented.

It mainly calls the attention to three important features: polarization of the lipid interphase, protrusion of the lipid molecules to the aqueous phase and water as a plasticizer element. All of them should be rigorously analyzed to have a realistic model for lipid membranes. The first one is related to water dipoles at the lipid interphase, the second with topology, in relation to head groups exposed to the water phase, the third is an important component in mechanical response.

The polarization brings about the idea that organization, mainly given by hydrogen bonding between water molecules themselves and with the different membrane groups, confers special mechanical and dynamical properties (see also Chap. 3). In this regard, when water is absorbed in solid, dehydrated phospholipids, it will act as a so-called “external plasticizer”, i.e. after gradual ingress of the solvent, the mobility and deformability of the membrane strongly enhances.

However, the limiting factor that ensures global integrity of the bilayer is its mechanical properties, which prevents its dissolution in an aqueous environment. What is essential for is that the mechanical properties, may also modulate permeants

and water permeation. This limiting factor arises from the entropic effect ensuring lamellar stability of lipid bilayers in water (Ben-Shaul 1995). This is therefore why solubility diffusion phenomena cannot be sustained with the classical assumption that the bilayer is an autonomous phase acting as a homogenous solvent for non polar solutes, only.

Water acts like a spacer when entering the headgroup region of lipids forcing free volume in the hydrocarbon chains leading to liquid phases. This criterion is used to explain why some molecules such as trehalose preserve membrane structure upon dehydration (Chap. 11).

Hydration enables an enhancement of the configurational space for additional degrees of freedom in water populations and most probably also in lipids (Ge and Freed 2003).

The debate on the validity of polarisation or protrusion models is not yet decided (Gordeliy 1996) but it seems that they are not independent, since protrusion changes polarity of the interphase by showing different groups to water. Moreover, the arguments discussed by Bagatolli in Chap. 5 suggest a distribution of different sites (or cavities) in the bilayer surface in which the fluorophore molecules can reside (Parasassi et al. 1997). Fluorophores are able to detect the local dielectric properties in which they are inserted. Thus, providing that the location in the membrane is known, they may be used to infer polar and non polar environments and to relate them to the presence of water. With this methodology, sites are characterized by a different number of dynamically restricted water molecules (Parasassi and Gratton 1995).

The average number of water molecules at the location of the LAURDAN fluorescent moiety 10 Å from the center of the bilayer (Antollini and Barrantes 1998) was estimated to be no more than two or three (Parasassi et al. 1997).

This few number of water molecules probably relates with those involved in the pore forming approach (Chap. 3). It is obvious to see that this number cannot physically define a pore, in the classical way described above, but rather defects of packing of nanomolecular dimensions, either in the acyl chain region or in the polar head groups, into which water may be organized. Water present in defects (Nagle and Tristram-Nagle 2000), illustrated by gaps in lipid film layers (see Fig. 2.4 in Chap. 2), form as irregularities in lamellar structure and because of imperfect bilayer alignment. Also protrusion may be considered a defect in which water polarization is changed.

The heterogeneity reported by these probes inserted in natural membrane systems could be interpreted in terms of distinct "structured water domains" (Almaleck et al. 2013; Heimburg 2010), not exclusively related to lipid packing, but to the combined ability of different membrane constituents to generate areas of different water content and dynamics. The dimension of these areas are of at most two to five water molecules as discussed in Chap. 9.

These considerations open the question formulated by Arsov in Chap. 6: *what about water molecules farther away from the membrane?*. This would be water beyond the water hydration hard core shell immobilized by polar head groups described Tristram Nagle,

How far does the influence of the membrane surface propagates into the water and what are the manifestations of such propagation? (Berkowitz and Vácha 2012)

These questions suggest that water beyond the hydration shell of the headgroups or near groups less abide for water (non polar residues) of the lipid structure is labile and could be perturbed easily by solutes in the aqueous phase. The properties of this kind of water could be relevant for membrane response in terms of the concept of "responding structure" coined by Sparr and Wennerström (2001). In this regard, the impact of hydration beyond the hydration water on the function of biomembranes should be discussed in terms of the lability of the solvent structure facing membrane surfaces of different polarities (i.e. polar or non polar groups). In thermodynamic terms, the lability is related to excess free energy, (surface tension) that is the driving force for insertion of compounds from the water phase into the membrane.

Results obtained by Arsov in Chap. 6 by attenuated total reflection Fourier transform infrared (ATR-FTIR) spectroscopy show that perturbation extends through several hydration layers beyond the first hydration shell. Consequently, water in confined membrane environments can be different than in the bulk.

In this chapter, Arsov defines different water species such as free water (bulk-like, far water), perturbed water (intermediate, freezable interlamellar water), and interfacial water (bound, buried, neighboring, non-freezable interlamellar water) (Kiselev et al. 1999; Kodama et al. 2001; Murzyn et al. 2006; Pinnick et al. 2010; Debnath et al. 2010). Such classification has been introduced very early also for hydration of proteins and peptides (Kuntz and Kauzmann 1974) and can be based on different attributes, such as water distance from the bilayer, water hydrogen bonding (HB) characteristics, as well as dynamic and thermodynamic properties.

The interfacial water is represented by water molecules that directly interact with lipids or reside in the interface region, while the free water denotes putative bulk-like molecules. The perturbed water corresponds to water in the transition region whose properties are still influenced by the presence of lipid membranes. It is concluded that the water structure is perturbed throughout the whole interlamellar space with thickness of about 1.8 nm in DMPC (Nagle and Tristram-Nagle 2000).

With the venue of computational calculations, water has been considered as a component in terms of stability, and different models for water structure (specifically the intermolecular interactions by hydrogen bondings) has been used (Berkowitz et al. 2006; Berkowitz and Vácha 2012; Bhide and Berkowitz 2005).

In this context, recently, the model visualizing the membrane as a low dielectric slab has been challenged in order to explain polar amino acid's penetration. Contrary to prediction of partition in non polar phases (White 1976; Wimley and White 1996; Preston Moon and Fleming 2011) charged aminoacids such as arginine are stabilized in the bilayer, which has been explained by means of molecular dynamics in terms of water pockets (Mac Callum et al. 2008; Herrera et al. 2012). In this regard, it has been recognized that water may penetrate the lipid bilayer reaching the region of the carbonyl groups (Simon and McIntosh 1986; Sovago et al. 2009; Disalvo and Frias 2013).

Alarcon et al. in Chap. 7 makes an interesting and novel evaluation of the water properties near different materials in comparison to lipid membranes. They investigate the properties of water buried in phospholipid membranes facing the lipid head groups and apolar alkyl chains (Malaspina et al. 2009).

Preliminary studies on membrane hydration consider that the effects of these interactions depend on the local environment. Results on the hydration and water penetration in phospholipid membranes indicate spatial distribution of water molecules around the different groups of the lipid molecules of the bilayer. The tendency of the water molecules to sacrifice the lowest hydrogen bond (HB) coordination as possible at extended interfaces reveals that the first hydration layers are highly oriented, in some situations even resembling the structure of hexagonal ice. A similar trend to maximize the number of HBs is shown to hold in cavity filling, with small subnanometric hydrophobic cavities remaining empty while larger cavities display an alternation of filled and dry states with a significant inner HB network.

An important conclusion relevant to biological phenomena is that the combination of different non-covalent interactions can produce clearly non-additive effects.

1.4 Water Beyond the Interphase: Water in Complex Systems

A more ambitious picture is proposed by Tsenkova in Chap. 8. She provides a framework for understanding changes in water giving a holistic description related to system functionality. Aquaphotomics, in addition to the other –omics disciplines, is based on the presumption that all the components of the system shape up the water matrix and would allow to describe the coupling between bio-chemical-physical perturbations and related changes in hydration structures. Water molecular conformations, for example dimers, trimers, solvation shells, etc., are known to contribute very specifically to its Near Infrared (NIR) spectrum. Direct evidence by means of FTIR spectroscopy shows that water band profiles are changed whether lipids are in the solid state, in the gel state after heating and cooling across the phase transition, or in the fluid state (Disalvo and Frias 2013). The different bands found in each case were assigned to different H-bonded water populations in agreement with the exposure of carbonyl groups.

1.5 Water and Surface Pressure: Its Implications in Membrane-Membrane and Membrane-Peptide Interactions

As pointed out in Chap. 2, the headgroup structural water, is considered to be a lower limit to measurements of tightly bound water. In monolayers, (Chap. 9) this limit is found at pressures corresponding to 40–45 $mN \bullet m^{-1}$, depending of the lipid head

group. This system allows to investigate further the hypothesis put forward by van Zoelen in liposome and to link permeability processes in bilayers with properties in the interphase region. The limit of packing given by the contact of the head group hydration water is defined as the cut off (critical) surface pressure, at which no effect of aminoacids, peptides or proteins on monolayer surface pressure is found (Chap. 9).

The perturbation of the surface pressure is produced when the area per lipid is just above 4 % larger than that corresponding to the hydration shell of the phospholipid head groups found in the cut –off, and therefore at lower surface pressures with respect to the cut off. The possibility that this area increase is related with the increase in water beyond the hydration shell, as anticipated by Bagatolli (Chap. 5) and studied by Arsov (Chap. 6) is discussed. The change in interfacial water activity is related with the surface pressure according to the Defay-Prigogine interphase model, which considers the interphase region as a bidimensional solution of head groups in water. As predicted by solution chemistry, the increase of surface pressure is independent of the protein nature but depends on the water surface state determined by the lipid composition.

With this background it is possible to analyse again the dynamics of different membrane processes such as solute and peptides penetration. Van Zoelen et al. (1976) claimed that in the isosmotic condition outflux and influx of water are counterbalanced by the outer solute concentration.

Liposomes and lipid vesicles swell when water penetrates until the chemical potentials of the solutions are equal inside and outside the structure (van Zoelen et al. 1976). While, the chemical potential in the outer media is given by the concentration of the components, those inside are determined by the concentration and the pressure exerted by the network of the bilayer on the solution. The viscoelastic properties of the bilayer may then contribute to the permeation processes. In the case of liposomes, the pressure can be exerted by the bilayer surrounding the internal solution. The cohesive forces maintaining the phospholipids in the structure contribute to this balance.

When permeant solutions are able to perturb the cohesive forces, more swelling would occur. At a 4 % volume increase in the swelling process of liposomes and vesicles results in a release of the liposomal content, such as ions which normally can not permeate the membrane, due to an increase in surface area (Evans and Skalak 1980). Thus, bilayer selectivity will vary according to the value of the reflection coefficient in the swelled structure a point also discussed by Nickels and Katsaras in Chap. 3.

The leakage produced at the critical volume increase is somehow congruent with the perturbation of the surface pressure produced when the area per lipid is above just 4 % larger than that corresponding to the hydration shell of the phospholipid head groups found in the cut –off.

Thus, variations of the membrane elasticity may be related to surface tension effects as inspected in monolayers and leakage cannot be necessary the result of membrane rupture. Instead, defects or fluctuations in the water lipid ratio along the membrane structure may explain the breakdown of the permeability barrier to ions (Deamer and Volkov 1995).

1.6 Interphase Water and Enzyme Activity

The studies by Damodaran in Chap. 10 extend further the relationship of monolayers with water activity, as a model experimental system for enzyme regulation.

A hypothesis is developed, which espouses that cells control activities of membrane-bound enzymes through manipulation of the thermodynamic activity of water in the lipid-water interfacial region. The hypothesis is based on the fact that the surface pressure of a lipid monolayer is a direct measure of the thermodynamic activity of water at the lipid-water interface. Accordingly, the surface pressure-dependent activation or inactivation of interfacial enzymes is directly related to changes in the thermodynamic activity of interfacial water.

Given that the physicochemical and structural properties of these enzymes are very different, it is inconceivable that all these enzymes would attain the catalytically active optimal conformation at a lateral mechanical force corresponding to a surface pressure of about 20 $mN \bullet m^{-1}$. This raises a very fundamental questions: Why at exactly this value? Is surface pressure really related to a *mechanical* lateral pressure exerted by the lipid layer or does it represent some other thermodynamic state or property of the interface that is essential for enzymes to adopt the catalytically most optimal structure?. Alternatively broader question are raised in terms of the evolutionary reasons for biology to choose the lipid-water boundary as the site for performing and/or controlling crucial biological reactions.

1.7 Life Without Water?

The question implicit in the origin of anhydrobiosis is if life can be preserved without water (Crowe, Chap. 11). It is known from a long time ago that one of the chief sites of damage in dehydration is the membrane, and some of them may be obviated by the production of certain sugars, particularly trehalose.

As discussed by Tristram-Nagle in Chap. 2, the main transition temperature of lipids (T_m) increased dramatically when the hydration level dropped below 20 wt.% water ($n_W = 12$). However, the lipid is maintained in the liquid-crystalline phase in the dry state if it is dried in the presence of trehalose.

Modifications of the gel state of hydrated phospholipids by trehalose can only be achieved if a drastic dehydration is performed in the presence of the sugar (Viera et al. 1993). The water activity in dimyristoylphosphatidylcholine (DMPC) decreases by 60 % when the lipid is dehydrated in the presence of trehalose concentrations higher than 0.02 M. Fourier transform infrared spectroscopy (FTIR) in these conditions denoted that trehalose binds to the carbonyl groups replacing 11 of 14 water molecules per lipid molecule. About four are displaced by changes in the water activity of the bulk solution, and seven by specific interactions with the phospholipids. In this last case, at least two of them are linked to the carbonyl group. This appears to be the cause of the decrease in the dipole potential of lipid monolayers spread on an air/water interface from 480 mV in pure water to 425 mV in 0.1 M trehalose (Luzardo et al. 2000).

Molecular dynamics simulations showed that trehalose binds to the phospholipid headgroups with its main axis parallel to the membrane normal. It establishes hydrogen bonds with the carbonyl and phosphate groups and replaces water molecules from the lipid headgroup. Notably, the number of hydrogen bonds (HBs) that the membrane made with its environment was conserved after trehalose binding. The HBs between lipid and trehalose have a longer lifetime than those established between lipid and water. The binding of the sugar does not produce changes either in the lipid area or in the lipid order parameter. The effect of trehalose on the dipole potential is in agreement with experimental results. The contribution of the different components to the membrane dipole potential was analyzed. It was observed that the binding of trehalose produces changes in the different components and the sugar itself contributes to the surface potential due to the polarization of its hydroxyl in the interface (Villarreal et al. 2004).

1.8 Contribution for a New Model for Lipid Membranes

Taken together, the approaches made by Crowe, Tsenkova and Damodaran extend the presence of water from the membrane interphase to the whole system. The details in the structure and properties of the membrane interphase is not constrained to a few nanometers near the lipids. Moreover, cells are now considered as crowded systems in which proximity between cell structure is linked by a few water layers. Thus, as an extension, the properties in the interphases can be visualized as the common interconnecting media. This new insight gives entrance to a holistic view of cells as entire complex systems in which membrane processes are essentials.

The traditional view of a membrane is an autonomous, rigid nonpolar slab sandwiched by bulk water phases implying isolation from the immediate surroundings. To fit membrane structure to the concept of complex systems, membrane should be considered as a non-autonomous phase. This means that the membrane (i.e. the lipid bilayer) is a phase whose properties depend on the phase which it is in contact with (i.e. water). This property has been denoted as responsive membranes by Sparr and Wennestrom (2001). This definition implies that the phenomena occurring at membrane level occurs with local or general changes in the membrane structure, that is, a response of the membrane to some component of the adjacent media, reflected in the thermodynamics and the kinetics of the protein–membrane interaction. The change in the membrane structure may be local with propagation to the whole structure in the plane and along the thickness with different degrees of cooperativity and synergism.

To decipher the biological phenomena in terms of membrane surface properties, the stability of the different arrays of water around the different membrane groups and its dynamical properties should be clarified. This includes namely: water as part of the membrane structure, the definition of the lipid interphases, the identification of the sites of hydration at the membrane surface; the synergism of their hydration

and its modulation according to the lipid species (usually found in biological membranes in terms of head group and fatty acid chains).

Details of water location and its properties in these restricted domains are scarce. The great variety of lipid composition and the multiple combinations in mixtures acquires relevance and functional meaning. As far as the properties of water microenvironments may be changed by the protrusion of the different polar moieties into the water phase, lipid species may generate new different water species each of them identified by the type of interaction they may have with its neighbor water molecules and/or chemical groups of the lipids. Thus, at this point, lipidomics approaches to aquaomics. In other words, lipid species would give an in-print on water with specific thermodynamic features for membrane response.

It is hoped that the discussions and ideas put forward in this book can be a stimulating start to study membrane phenomena in a more integrated approach in which water, in its different states and arrangements, appears as a common and unavoidable intermediary in biological response.

References

Al-Awqati Q (1999) One hundred years of membrane permeability: does Overton still rule? Nat Cell Biol 1(8):E201–E202

Almaleck H, Gordillo GJ, Disalvo A (2013) Water defects induced by expansion and electrical fields in DMPC and DMPE monolayers: contribution of hydration and confined water. Colloids Surf B Biointerfaces 102:871–878

Antollini SS, Barrantes FJ (1998) Disclosure of discrete sites for phospholipid and sterols at the protein-lipid interface in native acetylcholine receptor-rich membrane. Biochemistry 37:16653–16662

Bagatolli LA, Ipsen JH, Simonsen AC, Mouritsen OG (2010) An outlook on organization of lipids in membranes: searching for a realistic connection with the organization of biological membranes. Prog Lipid Res 49(4):378–389

Ben-Shaul A (1995) Molecular theory of chain packing, elasticity and lipid-protein interaction in lipid bilayers. In: Lipowsky R, Sackmann E (eds) Handbook of biological physics. Elsevier Science, North-Holland

Berkowitz ML, Vácha R (2012) Aqueous solutions at the interface with phospholipid bilayers. Acc Chem Res 45:74–82

Berkowitz ML, Bostick DL, Pandit S (2006) Aqueous solutions next to phospholipid membrane surfaces: insights from simulations. Chem Rev 106:1527–1539

Bhide SY, Berkowitz ML (2005) Structure and dynamics of water at the interface with phospholipid bilayers. J Chem Phys 123:224702

Chaplin MF (1999) A proposal for structuring of water. Biophys Chem 83:211–221

Chapman D, Urbina J, Keough K (1974) Studies of lipid-water systems using differential scanning calorimetry. J Biol Chem 249(8):2512–2521

Chapmann D (1971) Liquid crystalline properties of phospholipids and biological membranes. Symp Faraday Soc 5:163–174

de Gier J (1989) Chapter 4: Osmotic properties of liposomes. In: Benga G (ed) Water transport in biological membranes, vol I. CRC Press, Boca Raton

de Gier J, Mandersloot JG, Hupkes JV, McElhaney RNM, Van Beek NP (1971). On the mechanism of non electrolyte permeation through lipid bilayers and through biomembranes. Biochim Biophys Acta 223:610–618

Deamer DW, Volkov AG (1995) Chapter 8: Proton permeability of lipid bilayers. In: Disalvo EA, Simon SA (eds) Permeability and stability of lipid bilayers. CRC Press, Boca Raton, pp 161–178

Debnath A, Mukherjee B, Ayappa KG et al (2010) Entropy and dynamics of water in hydration layers of a bilayer. J Chem Phys 133:174704

Disalvo EA (1986) Permeation of water and polar solutes in lipid bilayers. Adv Colloid Interf Sci 29:141–170

Disalvo EA, De Gier J (1983) Contribution of aqueous interphases to the permeability barrier of lipid bilayer for non-electrolytes. Chem Phys Lipids 32:39–47

Disalvo EA, Frías MA (2013) Water state and carbonyl distribution populations in confined regions of lipid bilayers observed by FTIR spectroscopy. Langmuir 29(23):6969–6974

Disalvo EA, Lairion F, Martini F, Tymczyszyn E, Frías M, Almaleck H, Gordillo GJ (2008) Structural and functional properties of hydration and confined water in membrane interfaces. Biochim Biophys Acta 1778:2655–2670

Disalvo EA, Bouchet AM, Frias MA (2013) Connected and isolated CH populations in acyl chains and its relation to pockets of confined water in lipid membranes as observed by FTIR spectrometry. Biochim Biophys Acta 1828:1683–1689

Evans EA, Skalak R (1980) Mechanics and thermodynamics of biomembranes. CRC Press, Boca Raton, pp 67–91

Flory PJ (1969) Statistical mechanics of chain molecules. Interscience, New York

Ge MT, Freed JH (2003) Hydration, structure, and molecular interactions in the headgroup region of dioleoylphosphatidylcholine bilayers: an electron spin resonance study. Biophys J 85:4023–4040

Goñi FM (2014) The basic structure and dynamics of cell membranes: an update of the Singer-Nicolson model. Biochim Biophys Acta 1838(6):1467–1476

Goñi FM, Arrondo JLR (1986) A study of phospholipid 410 phosphate groups in model membranes by Fourier transform infrared 411 spectroscopy. Faraday Discuss Chem Soc 81:117–126

Gordeliy VI (1996) Possibility of direct experimental check up of the theory of repulsion forces between amphiphilic surfaces via neutron and X-ray diffraction. Langmuir 12:3498–3502

Gordeliy VI, Cherezov VG, Teixeira J (1996) Evidence of entropic contribution to “hydration” forces between membranes Part II. Temperature dependence of the “hydration” force: a small angle neutron scattering study. J Mol Struct 383:117–124

Griffith OH, Dehlinger PJ, Van SP (1974) Shape of the hydrophobic barrier of phospholipid bilayers (evidence for water penetration in biological membranes). J Membr Biol 15:159–192

Haines T, Liebovitch LS (1995) Chapter 6: A molecular mechanism for the transport of water across phospholipid bilayers. In: Disalvo EA, Simon SA (eds) Permeability and stability of lipid bilayers. CRC Press, Boca Raton, pp 137–160

Heimburg T (2010) Lipid ion channels (review). Biophys Chem 150(1–3):2–22

Herrera FE, Bouchet A, Lairion F, Disalvo EA, Pantano S (2012) Molecular dynamics study of the interaction of arginine with phosphatidylcholine and phosphatidylethanolamine bilayers. J Phys Chem B 116:4476–4483

Ipsen JH, Mouritsen OG, Bloom M (1990) Relationships between lipid membrane area, hydrophobic thickness, and acyl- chain orientational order. Biophys J 57:405–412

Israelachvili JN (1977) Refinement of the fluid-mosaic model of membrane structure. Biochim Biophys Acta 469:221–225

Israelachvili J, Wennerström H (1996) Role of hydration and water structure in biological and colloidal interactions. Nature 379(6562):219–225

Jendrasiak GL, Hasty JH (1974) The hydration of phospholipids. Biochim Biophys Acta 337(1):79–91

Jendrasiak GL, Smith RL, Shaw W (1996) The water adsorption characteristics of charged phospholipids. Biochim Biophys Acta 1279:63–69

Kedem O, Katchalsky A (1958) A thermodynamic analysis of the permeability of biological membranes to non-electrolytes. Biochim Biophys Acta 27:229–246

Kiselev M, Lesieur P, Kisselev A et al (1999) DMSO-induced dehydration of DPPC membranes studied by X-ray diffraction, small-angle neutron scattering, and calorimetry. J Alloys Compd 286:195–202

Kodama M, Kato H, Aoki H (2001) Comparison of differently bound molecules in the gel and subgel phases of a phospholipid bilayer system. J Therm Anal Calorim 64:219–230

Kuntz ID, Kauzmann W (1974) Hydration of proteins and polypeptides. Adv Protein Chem 28:239–345

Luzardo MC, Amalfa F, Nuñez AM, Díaz S, Biondi De Lopez AC, Disalvo EA (2000) Effect of trehalose and sucrose on the hydration and dipole potential of lipid bilayers. Biophys J 78(5):2452–2458

MacCallum L, Bennett WF, Tieleman DP (2008) Distribution of amino acids in a lipid bilayer from computer simulations. Biophys J 94:3393–3404

Malaspina DC, Rodriguez Fris JA, Appignanesi GA, Sciortino F (2009) Identifying a causal link between structure and dynamics in supercooled water. Europhys Lett 88:16003

Mathai JC, Tristram-Nagle S, Nagle JF (2008) Structural determinants of water permeability through the lipid membrane. J Gen Physiol 131(1):69–76

McElhaney RN, de Gier J, van der Neut-Kok ECM (1973) The effect of alterations in fatty acid composition and cholesterol content on the nonelectrolyte permeability of Acholeplasma laidlawii B cells and derived liposomes. Biochim Biophys Acta 298:500–512

McIntosh TJ, Simon SA, Dilger JP et al (1989) Chapter 1: Location of water-hydrocarbon interface in lipid bilayers. In: Benga G (ed) Water transport in biological membranes, vol 1. CRC Press, Boca Raton

Murzyn K, Zhao W, Karttunen M et al (2006) Dynamics of water at membrane surfaces: effect of headgroup structure. Biointerphases 1:98–105

Nagle JF, Tristram-Nagle S (2000) Structure of lipid bilayers. Biochim Biophys Acta Rev Biomembr 1469(3):159–195

Overton E (1889) Über die allgemeinen osmotischen Eigenschaften der Zelle, ihre vermutlichen Ursachen und ihre Bedeutung für die Physiologie. Vierteljahrsschr Natur-forsch Ges Zürich 44:88–135

Parasassi T, Gratton E (1995) Membrane lipid domains and dynamics as detected by LAURDAN fluorescence. J Fluoresc 5:59–69

Parasassi T, Gratton E, Yu WM, Wilson P, Levi M (1997) Two-photon fluorescence microscopy of laurdan generalized polarization domains in model and natural membranes. Biophys J 72:2413–2429

Pinnick ER, Erramilli S, Wang F (2010) Computational investigation of lipid hydration water of L α 1-palmitoyl-2-oleoyl- sn -glycero-3-phosphocholine at three hydration levels. Mol Phys 108:2027–2036

Preston Moon C, Fleming KG (2011) Side-chain hydrophobicity scale derived from transmembrane protein folding into lipid bilayers. Proc Natl Acad Sci U S A 108(25):10174–10177

Simon SA, McIntosh TJ (1986) Depth of water penetration into lipid bilayers. Methods Enzymol 127:511–521

Singer SJ, Nicolson GL (1972) The fluid mosaic model of the structure of cell membranes. Science 175(23):720–723

Sovago M, Vartiainen E, Bonn M (2009) Observation of buried water molecules in phospholipid membranes by surface sum-frequency generation spectroscopy. J Chem Phys 131:161107–161111

Sparr E, Wennerström H (2001) Responding phospholipid membranes—interplay between hydration and permeability. Biophys J 81(2):1014–1028

Ti Tien H, Ottova AL (2001) The lipid bilayer concept and its experimental realization: from soap bubbles, kitchen sink, to bilayer lipid membranes. J Membr Sci 189:83–117

Träuble H (1971) The movement of molecules across lipid membranes: a molecular theory. J Membr Biol 4(1):193–208

Van Zoelen EJJ, Blok MC, De Gier J (1976) An improved method for the description of non-electrolyte permeation through liposomes, based on irreversible thermodynamics. Biochim Biophys Acta Biomembr 436(2):301–306

Viera LI, Alonso-Romanowski S, Borovyagin V, Feliz MR, Disalvo EA (1993) Properties of gel phase lipid-trehalose bilayers upon rehydration. Biochim Biophys Acta 1145(1):157–167

Villarreal MA, Díaz SB, Disalvo EA, Montich GG (2004) Molecular dynamics simulation study of the interaction of trehalose with lipid membranes. Langmuir 20:7844–7851

White SH (1976) The lipid bilayer as a "solvent" for small hydrophobic molecules. Nature 262:421–422

Wimley C, White SH (1996) Experimentally determined hydrophobicity scale for proteins at membrane interfaces. Nat Struct Biol 3:842–848

Yeagle PL (2004) The structure of biological membranes, 2nd edn. CRC Press, Boca Raton (FL).

Chapter 2
Use of X-Ray and Neutron Scattering Methods with Volume Measurements to Determine Lipid Bilayer Structure and Number of Water Molecules/Lipid

Stephanie Tristram-Nagle

Abstract In this chapter I begin with a historical perspective of membrane models, starting in the early twentieth century. As these membrane models evolved, so did experiments to characterize the structure and water content of purified lipid bilayers. The wide-spread use of the X-ray gravimetric, or Luzzati method, is critically discussed. The main motivation of the gravimetric technique is to determine the number of water molecules/lipid, n_W, and then derive other important structural quantities, such as area/lipid, A_L. Subsequent experiments from the Nagle/Tristram-Nagle laboratory using X-ray and neutron scattering, first determine A_L and then calculate n_W, using molecular lipid V_L and water V_W volumes. This chapter describes the details of our volume experiments to carefully measure V_L. Our results also determine n_W', the steric water associated with the lipid headgroup, and how our calculated value compares to many literature values of tightly-associated headgroup water.

Keywords Waters/lipid • Hydration • Lipid bilayer • X-ray scattering • Neutron scattering

Abbreviations

DSC	Differential scanning calorimetry
NMR	Nuclear magnetic resonance
EPR	Electron spin resonance
FTIR	Fourier transform infrared resonance
Tm	Main transition melting temperature
n_W	Number of waters/lipid

S. Tristram-Nagle (✉)
Biological Physics Group, Physics Department, Carnegie Mellon University, Pittsburgh, PA 15213, USA
e-mail: stn@cmu.edu

E.A. Disalvo (ed.), *Membrane Hydration*, Subcellular Biochemistry 71,
DOI 10.1007/978-3-319-19060-0_2

n_W'	Steric number of waters/lipid
A_L	Area/lipid
V_L	Molecular volume/lipid
V_W	Molecular volume/water
MLVs	Multilamellar vesicles
ULVs	Unilamellar vesicles
D, D-space	X-ray lamellar D-spacing
d, d-space	X-ray wide-angle chain spacing
η	Fluctuation parameter
K_C	Bending modulus
B	Bulk modulus
u_n	Vertical displacement
$I(q_z)$	X-ray intensity
$\|F(q_z)\|$	Form factor
MD simulation	Molecular dynamics simulation
$2D_C$	Hydrocarbon thickness
D_B	Bilayer thickness
D_H'	Headgroup thickness
interdig.	Interdigitated
DPPC	Dipalmitoylphosphatidylcholine
DSPC	Distearoylphosphatidylcholine
DHPC	Dihexadecanoyl-phosphatidylcholine
DLPE	Dilauroylphosphatidylethanolamine
DMPC	Dimyristoylphosphatidylcholine
DMPE	Dimyristoylphosphatidylethanolamine
DLPC	Dilauroylphosphatidylcholine
DOPC	Dioleoylphosphatidylcholine
DOPS	Dioleoylphosphatidylserine
EggPC	Egg phosphatidylcholine
POPC	Palmitoyloleoylphosphatidylcholine
SOPC	Stearoyloleoylphosphatidylcholine
diC22:1PC	Dierucoylphosphatidylcholine
18:0:22:5PC	Stearoyldocosapentaenoylphosphatidylcholine
18:0-22:6PC	Stearoyldocosahexaenoylphosphatidylcholine
diphytanoylPC	Diphytanoylphosphatidylcholine
DLPG	Dilauroylphosphatidylglycerol
DMPG	Dimyristoylphosphatidylglycerol
POPG	Palmitoyloleoylphosphatidylglycerol
SOPG	Stearoyloleoylphosphatidylglycerol
DOPG	Dioleoylphosphatidylglycerol
TMCL	Tetramyristoylcardiolipin
DMPS	Dimyristoylphosphatidylserine

2.1 Historical Perspective

The study of lipid membranes, the underlying structure of all cell membranes, began near the beginning of the twentieth century (Swart 1907). The phospholipid bilayer was first proposed by Gorter and Grendell in 1925, by comparing monolayer areas of extracted red blood cell lipids with calculated cell surface areas (Gorter and Grendel 1925). In 1935, Hugh Davson and James Danielli proposed a model of the cell membrane in which the phospholipid bilayer lies between two layers of globular protein (Danielli and Davson 1935). Twenty-five years later, J. David Robertson determined that the dark bands observed in electron microscopy on either side of the membrane were the lipid headgroups and associated proteins of two apposed lipid monolayers, comprising a rigid "unit cell" (Robertson 1960). This static picture of a membrane was rejected 10 years later due to experiments by Frey and Edidin who fused two fluorescently labeled cells and watched as the dye populations mixed (Frye and Edidin 1970). The results of this experiment were key in the development of the "fluid mosaic" model of the cell membrane by Singer and Nicolson, where membrane lipids and proteins are viewed as highly mobile (Singer and Nicolson 1972). More recently, the idea of transient or permanent membrane domains (rafts) containing cholesterol and detergent-resistant proteins diffusing within the fluid bilayer has become the leading paradigm (Simons and Toomre 2000). As these models evolved, many precise biophysical investigations of the thermotropic and lyotropic properties of the underlying lipid bilayer were carried out using NMR, differential scanning calorimetry, FTIR, X-ray diffraction, centrifugation and fluorescence. Since natural membranes exist in a fully hydrated environment, the water component is necessarily an important part of the lipid structure. Indeed, without water, life is impossible. In this chapter, I will discuss some early experiments to obtain the total number of water molecules/lipid in stacked membranes, n_W, and other experiments that attempted to obtain the number of tightly bound water molecules/lipid, n_W'. The main focus will be on the use of scattering techniques: early experiments with X-ray diffraction, and our more modern method of X-ray diffuse scattering, sometimes combined with neutron scattering, that first obtains the fluid phase area/lipid and then calculates n_W and n_W' from known equations.

2.2 Gravimetric, or Luzzati Method

Why should we be concerned about n_W, number of waters/lipid? The main reason is that if lipids become too dehydrated, their physical and structural properties change. I.e., the water is actually part of the structure of the hydrated lipid. Then the question is, how much water is needed to maintain the equilibrium lipid structure and properties? In the 1960s, a pioneer in this field was Dennis Chapman who used differential scanning calorimetry (DSC), nuclear magnetic resonance (NMR),

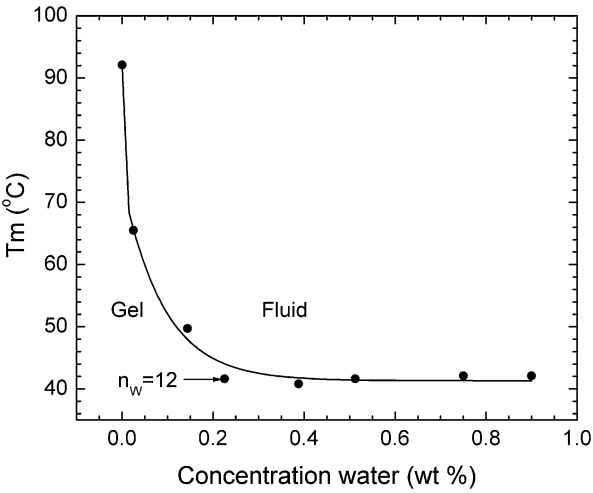

Fig. 2.1 Melting temperature (Tm) of DPPC vs. water concentration (wt %) obtained by DSC (Redrawn with permission from Fig. 3 (Ladbrook et al. 1968))

electron spin resonance (EPR), and Fourier transform infrared resonance (FTIR) to characterize the lyotropic behavior of lipid bilayers. In Fig. 2.1**,** Chapman's DSC data show the effect of the water content on the main melting transition temperatures (Tm's) of DPPC.

As shown in Fig. 2.1, when the hydration level dropped below 20 wt% water ($n_W = 12$), the measured Tm (main chain melting) increased dramatically. This indicates that the fluid phase of dipalmitoylphosphatidylcholine (DPPC) requires at least 12 water molecules for stability. Thus, in this relatively simple experiment, where careful weighing of water and lipid is required, large changes in lipid physical properties are observed at limiting water content, emphasizing the importance of adequate water in the lipid structure.

Another pioneer in the field of lipid bilayers is Vittorio Luzzati, who studied lipid bilayer structure using X-rays at about the same time that Chapman was using DSC and spectroscopic methods. When membranes are stacked to form an array, their X-ray diffraction pattern consists of Bragg reflections, which indicates that the array consists of membranes lying with their planes parallel, that are spaced relatively regularly. This occurs spontaneously when dried lipids are thoroughly mixed with water, forming onion-like structures, called multilamellar vesicles (MLVs). The D-spacing of the array is determined by the bilayer thickness plus the water between the bilayers. The amount of water between bilayers is determined by a balance of forces: in the gel phase there is an attractive van der Waals force and a repulsive hydration force, while in the fluid phase there is also a repulsive fluctuation force (Petrache et al. 1998a). A typical example of an X-ray pattern from an MLV consisting of the gel phase lipid, DPPC, is shown in Fig. 2.2.

The lamellar D-spacing is foundational to the gravimetric, or Luzzati method. This method entails: (1) drying the lipid completely before weighing, (2) weighing precise amounts of dried lipid with water, (3) equilibrating the lipid/water mixture,

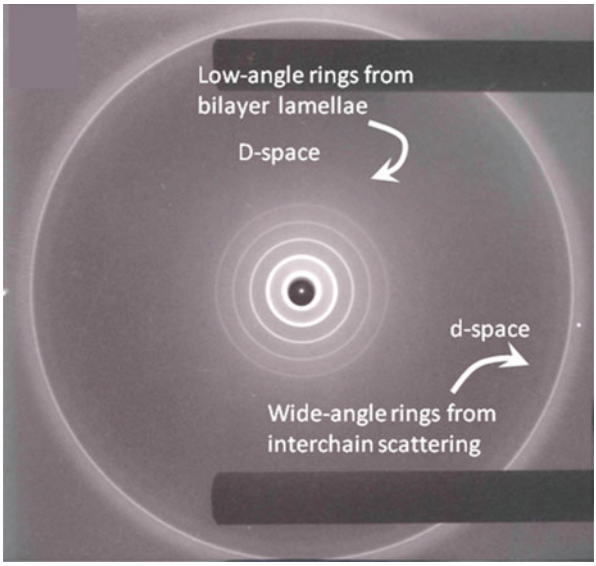

Fig. 2.2 X-ray diffraction pattern showing low-angle, central rings used to obtain the lamellar D-spacing, and wide-angle peripheral rings, using to obtain the d-spacing, distance between chains. Film data of DPPC at room temperature (*RT*) obtained by Prof. Roy Worthington at the Cornell High Energy Synchrotron Source (CHESS) in 1992. *Dark shadows* are from the film holder

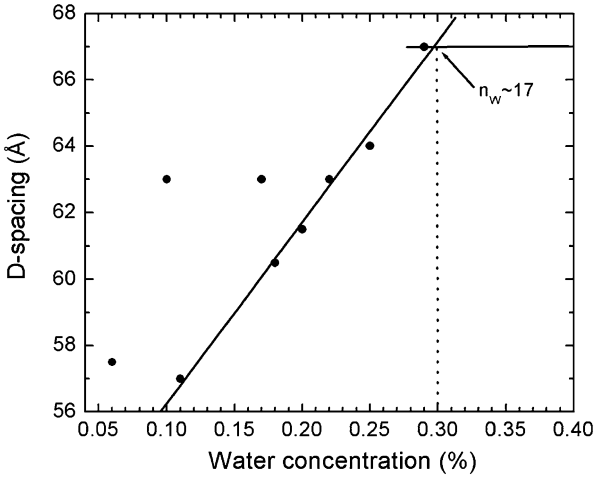

Fig. 2.3 D-spacing of DPPC at 20 °C vs. water concentration (wt %) obtained by X-ray diffraction (Redrawn with permission from Table 1 (Tardieu et al. 1973))

sometimes at high temperatures, to hydrate thoroughly, (4) X-raying the resulting multilamellar sample to obtain a D-spacing, or distance between layers, that includes both the lipid thickness and associated water, (5) plotting D-spacing vs. water concentration, (6) determining the fully hydrated water concentration where the D-spacing levels off by extrapolation, and (7) converting weight percent to n_W using the molecular weights of lipid and water. An example of results from the gravimetric method is shown in Fig. 2.3 for the same DPPC lipid as in Fig. 2.2.

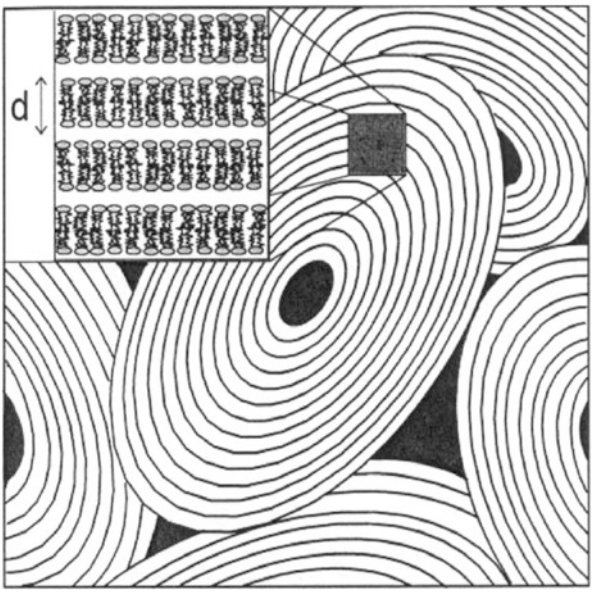

Fig. 2.4 An illustration of the formation of water pools (*black*), in the center of MLVs and between MLVs (Reproduced with permission from Fig. 3 (Koenig et al. 1997))

There are several problems with the gravimetric method. The greatest problem has been pointed out by Gawrisch et al. (Koenig et al. 1997). Their previous studies on PC lipids in the Lα phase suggested that only the first 15 water molecules per lipid are homogeneously incorporated (Gawrisch et al. 1985). When more water is added, instead of locating neatly between the bilayers in a MLV, pools of water form, causing gradual changes in the morphology of the sample (Klose et al. 1988). This problem was discussed in (Nagle and Tristram-Nagle 2000) and is shown in the cartoon in Fig. 2.4. Formation of water pools can wreak havoc on the gravimetric method, since added water does not contribute to the measured D-spacing if the added water locates in a pool. Notice that the n_W determined in Fig. 2.3 is larger than that determined using DSC in Fig. 2.1 due to this artefact. Then, there are several other problems that add to the errors in this method. First, the lipid component must be completely anhydrous before weighing. It is difficult to remove the last 1–2 water molecules as has been measured (Jendrasiak and Hasty 1974), which normally is not a problem, but when accurate numbers are required, then this introduces an error of 10 %. Second, the lipid has to be precisely weighed, as does the water, so highly accurate balances are required. Human error can occur during this step, so many repetitions with different sample sizes are required to obtain accurate concentrations. Third, the sample must be hydrated by vortexing and temperature cycling. Evaporation of water can occur during this step if the sample is not properly sealed. Fourth, the sample must be transferred to a container that allows X-rays to pass through it. Usually this is a glass capillary, or the Luzzati

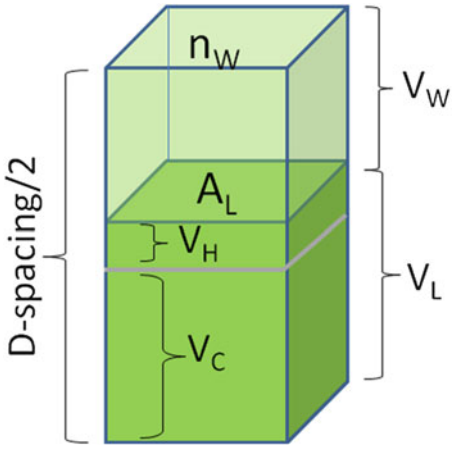

Fig. 2.5 Drawing showing V_L (*darker green*) with its associated water V_W (*transparent green*). V_H = volume/headgroup and V_C = volume/hydrocarbon. These volumes represent one monolayer in the bilayer which contributes to ½ lamellar D-spacing

cell where the sample is contained between mica or mylar windows. Evaporation of water can occur during the transfer and sealing of the X-ray container. Fifth, even with temperature cycling and vortexing, the MLV may not be at equilibrium with its surrounding water; the onion-skin structure can trap water molecules and prevent the maximum swelling from occurring, as if an osmotic pressure were being applied, especially in the fluid phase. Finally, in order to estimate the full water component using the gravimetric method, it is necessary to fit linearly the D-spacings on the approach to full hydration and in the plateau region, and find their intersection (see Fig. 2.3). There can be errors in the intersection value, due to noisy data, and an increasing slope after "full" hydration has been reached.

In the above methods, n_W is obtained first, and then the area/lipid (A_L) is calculated as the desired result. The equation that is used is:

$$A_L = 2\left(V_L + n_W V_W\right)/D \tag{2.1}$$

where V_L and V_W are the lipid and water molecular volumes (Å^3), respectively, at the temperature of the experiments, and D is the fully hydrated D-spacing (Å). This equation is shown pictorially in Fig. 2.5. In our laboratory we have always measured V_L using either the combined technique of differential scanning dilatometry (Nagle and Wilkinson 1978) and neutral flotation (Wiener et al. 1988), neutral flotation alone, or differential scanning densimetry with a modern Anton-Paar DMA 5000 M densimeter (Tristram-Nagle et al. 2010). Several other groups simply calculate V_L by adding measured (or calculated) volumes of the lipid's component groups. The latter practice is a source for error in obtaining n_W and A_L; V_L should be measured at the temperature of the experiments whenever possible. More details about our volume measurements will be given in Sect. 2.6.

2.3 Obtaining A_L: Gel Phase

Obtaining the area/lipid, A_L, is straightforward using X-ray diffraction techniques in the gel phase of a bilayer. In addition to low-angle scattering that produces the D-spacing discussed above, lipid bilayers also scatter in the wide-angle region due to their chain-chain correlation, with d-spacing 4–5 Å. Using the wide-angle d-spacings, A_L is calculated with the equation:

$$A_L = 2A_C/\cos\theta \tag{2.2}$$

where A_C is the area/chain (Å^2) and θ is the chain tilt angle. Details on how to obtain A_C from the wide-angle spacings can be found in Levine (1973) and Tristram-Nagle et al. (1993). Since the headgroup area is larger than the combined area of the two hydrocarbon chains beneath it, the chains tilt in order to maximize van der Waals interactions between them (Nagle 1976). In the gel phase, the lipid chains are in the *all-trans* state, which are essentially straight chains. The chain scattering is confined to Bragg rods in the wide-angle region; while the 2,0 rod lies on the equator, the 1,1 rod is lifted up due to the chain tilt. The chain tilt is obtained by first measuring the angle off the equator of the 1,1 wide-angle rod (see Fig. 2.6 for an example) in a fully hydrated, oriented gel phase sample. The chain tilt angle is calculated as in (Tristram-Nagle et al. 1993) using the angle η as drawn in Fig. 2.6. Notice that in an oriented gel phase pattern, low-angle scattering is along the q_z (vertical) axis, and wide-angle scattering has a q_r (horizontal) component, compared to the isotropic scattering in the MLV data (shown in Fig. 2.2).

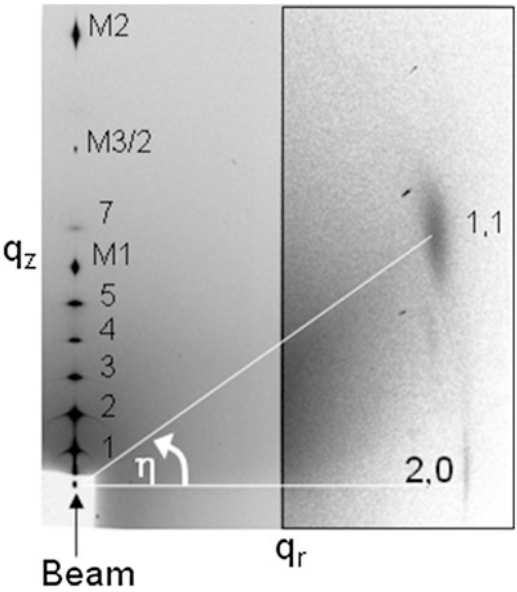

Fig. 2.6 Dimyristoylphosphatidylcholine (DMPC) low-angle lamellar orders are numbered in increasing q_z, while mica peaks are labeled with M. Wide-angle peaks (2,0 and 1,1) are shown to the right with a higher contrast. The angle η is directly related to the chain tilt angle θ (Reproduced with permission from Fig. 4 (Tristram-Nagle et al. 2002))

2.4 Obtaining A_L: Fluid Phase

In the fluid phase, the chains are disordered with 4 gauche rotamers per chain (Nagle 1980; Mendelsohn et al. 1991). A gauche rotamer is a rotation of 120° about a C-C single bond; when there are two or three gauche rotamers in a row, it is referred to as a kink in the chain. Although a theory from the liquid-crystal literature obtains A_L using a disordered wide-angle pattern (Levine 1973; Mills et al. 2008), the precision of this method is less than that of the gel phase A_L wide-angle determination described above. A more precise A_L is obtained by using low-angle X-ray scattering (LAXS) that results from fully hydrated, oriented lipid membranes as developed in the Nagle/Tristram-Nagle lab ((Tristram-Nagle and Nagle 2004), sometimes combined with neutron scattering from isotropic, unilamellar vesicles (ULV) (Kučerka et al. 2008). The basic principle of this method is to obtain the bilayer thickness, without its associated water. Then, by also measuring V_L, A_L is directly obtained using two equations, either separately or combined:

$$A_L = V_C/D_C \text{ (X-rays) or } A_L = 2V_L/D_B \text{ (neutrons)} \qquad (2.3, 2.4)$$

where D_C is the hydrocarbon thickness and D_B is the bilayer thickness without water. V_C is determined by subtracting the headgroup volume, V_H, from V_L. Headgroup volume is determined using gel phase data as described in (Tristram-Nagle et al. 2002) and we assume that V_H doesn't change with temperature. D_C is determined by fitting fluid phase X-ray data to the Scattering Density Profile (SDP) fitting program. These thicknesses are depicted in Fig. 2.7c, which also shows the total electron density profile of a lipid bilayer (**b**) and its component group probabilities (**a**).

Neutrons use a different measure of bilayer thickness, D_B, which is defined as the Gibbs dividing surface of water. As shown in Fig. 2.7, D_B is in the headgroup region, while D_C is closer to the bilayer center. Using the SDP program, both X-ray and neutron scattering data can be fit simultaneously through the Fourier transform to a model of the bilayer with component groups. An example of these types of data are shown for the lipid diphytanoylPC in Fig. 2.8.

In that work $A_L = 80.5$ Å^2 and $n_W = 37$ (Tristram-Nagle et al. 2010). By combining Eqs. 2.3 and 2.4 during the fit to both X-ray and neutron data, a compromise A_L was determined, which is between a slightly larger A_L using X-ray data alone (83 Å^2) and a slightly smaller A_L using neutron data alone (78 Å^2). When studying another lipid, dioleoylphosphatidylcholine (DOPC), our lab similarly found a larger area (72.4 Å^2) using X-rays alone (Pan et al. 2008a; Kučerka et al. 2005b) compared to 66.5 Å^2 using neutrons alone (Gallova et al. 2008). When X-rays and neutron data were analyzed simultaneously using the SDP program, DOPC $A_L = 67.4$ Å^2 (Kučerka et al. 2008). Since areas are used to determine n_W, this variability represents a 16–20 % error. Although for these two examples, the neutron scattering data yielded smaller areas, for the case of DPPC in the fluid phase, the areas were the same for X-rays and neutrons (Kučerka et al. 2008).

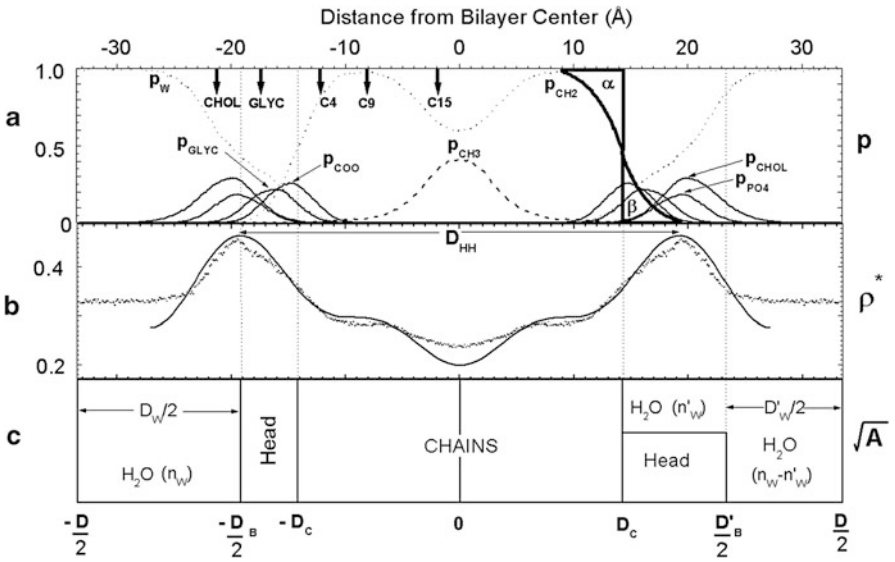

Fig. 2.7 Three representations of the structure of DPPC bilayers in the Lα fluid phase: (**a**) Probability distribution functions for component groups (from simulations). Abbreviations: *W* water, *Glyc* glycerol, *Chol* choline, *COO* carbonyl, CH_2 methylenes, CH_3 terminal methyl and PO_4 phosphate. The equality of the areas α and β determines the Gibbs dividing surface, or edge, of the hydrocarbon region. (**b**) Electron density profiles from X-ray data (*solid line*) and from simulations (*dotted line*). (**c**) Two volumetric pictures: *left*, a 3-compartment model and *right*, a more realistic model of the interfacial headgroup region (Reproduced with permission from Fig. 2 (Nagle and Tristram-Nagle 2000))

2.5 Details of the X-Ray Diffuse Scattering Method

While it is fairly straightforward to obtain neutron scattering data from ULV by methods described in (Lewis and Engelman 1983; Kučerka et al. 2004), it took our laboratory about 4 years to develop the data collection and analysis methods that use oriented, fully hydrated lipid membranes (Lyatskaya et al. 2001; Tristram-Nagle and Nagle 2004). Unlike gel phase X-ray diffraction where 7–10 lamellar orders are observed, X-ray scattering from fluid phase, fully hydrated MLV produces only two lamellar orders, with the h = 2 quite weak, due to the fluctuations and undulations caused by thermal energy. There is disorder both within a single bilayer as well as disorder caused by correlations between fluctuating bilayers (Guinier 1963). This causes loss of lamellar diffraction orders, as well as loss of intensity in the remaining two orders, which redistributes to diffuse scattering between peaks. This creates problems for structure determination, in that the resolution is quite poor. If a negatively charged lipid is present, there are no lamellar orders at all, since the lipid lamellae unbind from each other. What many labs have done is to dehydrate fluid phase bilayers, in order to produce more lamellar orders. While this method does

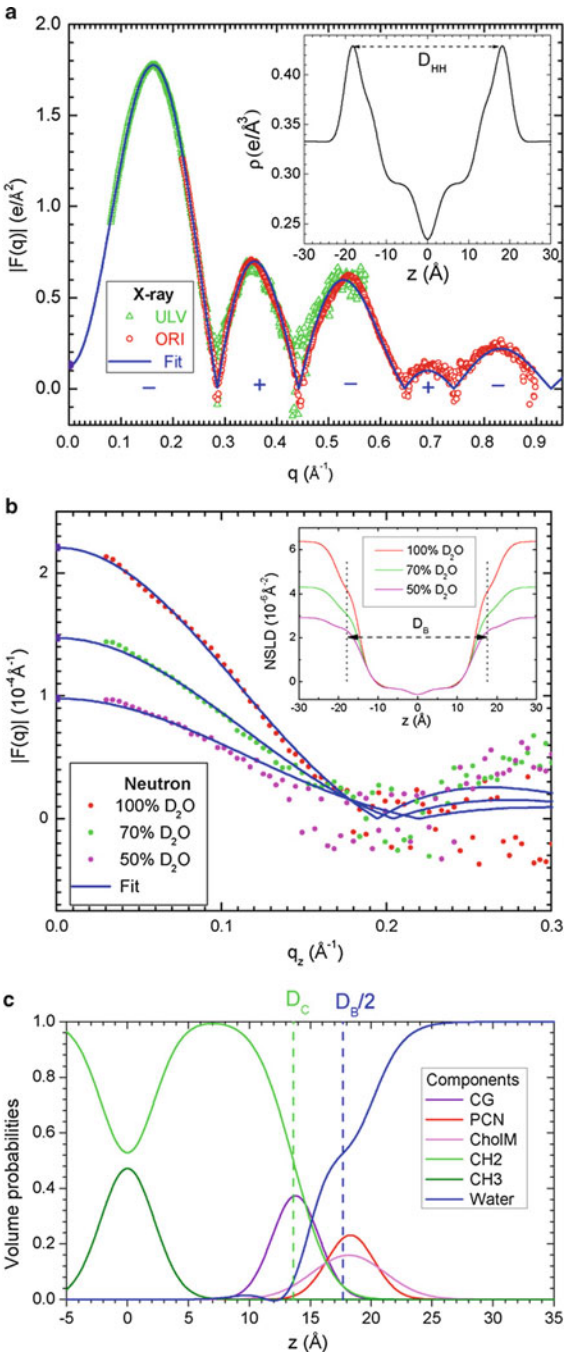

Fig. 2.8 (**a**) Absolute X-ray form factors for diphytanoylPC at 30 °C. ULV (*green*) and oriented (*red*) data are both fit to a model of a bilayer (*blue*) using the SDP program. *Inset* shows the corresponding electron density profile (Reproduced with permission from Fig. 6 (Tristram-Nagle et al. 2010)). (**b**) Absolute neutron form factors for ULV of diphytanoylPC at 30 °C in three concentrations of D_2O/H_2O. *Inset* shows the corresponding scattering length density profiles, with D_B indicated by *vertical, dotted lines* (Reproduced with permission from Fig. 7 (Tristram-Nagle et al. 2010)). (**c**) Volume probabilities for the components of the SDP model: CG (carbonyl + glycerol); PCN (phosphate $+2CH_2 + N$); CholM ($(CH_3)^3$ on N); CH_2 (chain methylenes); CH_3 (chain terminal methyls); and water. The probabilities are symmetric about the bilayer center at z = 0. The *dotted green line* is located at D_C, the Gibbs' dividing surface for the hydrocarbon region, and the *dashed blue line* is located at $D_B/2$, the Gibbs dividing surface for water (Reproduced with permission from Fig. 8 (Tristram-Nagle et al. 2010))

succeed at producing more orders, thermal fluctuations are usually lost, removing the lipids further from their biologically relevant state.

In fact, our lab started with this method, applying a correction to the obtained scattering, due to the fluctuations that are present when bilayers are only slightly dehydrated, but still close to full hydration (Zhang et al. 1994, 1995). We model the disorder based on liquid-crystal theory (Caillé 1972; de Gennes and Prost 1993), which, when compared to paracrystalline theory (Hosemann and Bagchi 1962), is a better fit to the diffuse X-ray scattering data that emanates from fluctuating bilayers (Zhang et al. 1996). In our original method, samples were MLVs in X-ray glass capillaries, producing an isotropic pattern, similar to that shown in Fig. 2.2 for gel phase DPPC, but with fewer lamellar orders due to fluctuations. Using a high-resolution synchrotron X-ray setup to resolve peak shape of lamellar Bragg orders, the thermal fluctuations were analyzed using the modified Caillé analysis (Zhang et al. 1996). With this we calculated η, which is a combined fluctuation parameter of the bending modulus, K_C, and the bulk modulus, B (Nagle and Tristram-Nagle 2000) (and references therein). While K_C is a measure of the energy required to bend a single membrane, B is a measure of interaction energy between bilayers in a stack (see Fig. 2.9). The theory is based upon a free energy function shown in Eq. 2.5.

The theory quantifies the displacement, u_n, of a fluctuating bilayer from its flat position, which is used in the correlation function that then obtains the structure factor of a fluctuating bilayer. While isotropic samples can only provide η, the combined fluctuation parameter, oriented samples can provide K_C and B separately (Lyatskaya et al. 2001). In the late 1990s, our lab succeeded in obtaining well-oriented thin membrane films produced by a method pioneered by Tristram-Nagle (Tristram-Nagle et al. 1993; Tristram-Nagle 2007). A diagram of this sample is shown in Fig. 2.10.

It was initially difficult to hydrate lipid samples to full hydration through the vapor, which was referred to as the vapor pressure paradox (Rand and Parsegian 1989). Even gel phase lipids, which require less water than fluid phase lipids, did

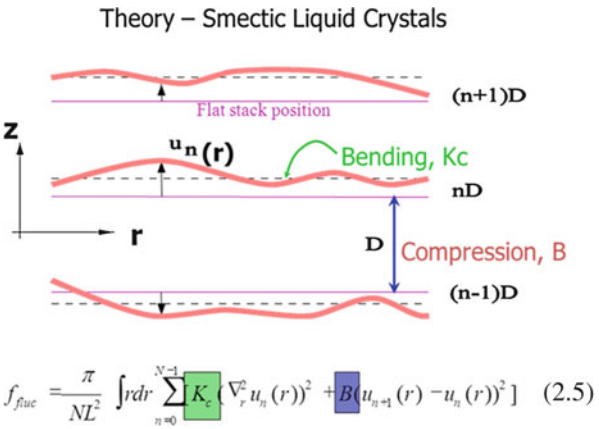

Fig. 2.9 Diagram of smectic liquid crystal theory for a fluctuating stack of bilayers and Eq. 2.5 showing how K_C and B are related to the displacement u_n in the free energy functional (de Gennes and Prost 1993). The displacement, u_n, is evaluated in the radial r direction

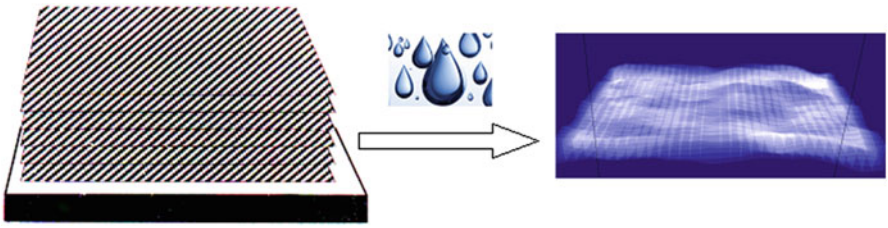

Fig. 2.10 An oriented stack *(left)*, 10 μ thick, consisting of 1800 bilayers, hydrates through the vapor in a well-insulated chamber producing thermal fluctuations near full hydration in the lipid fluid phase. Fluctuating bilayers were analyzed using a Monte Carlo program (Gouliaev and Nagle 1998) that was used to create this image *(right)*

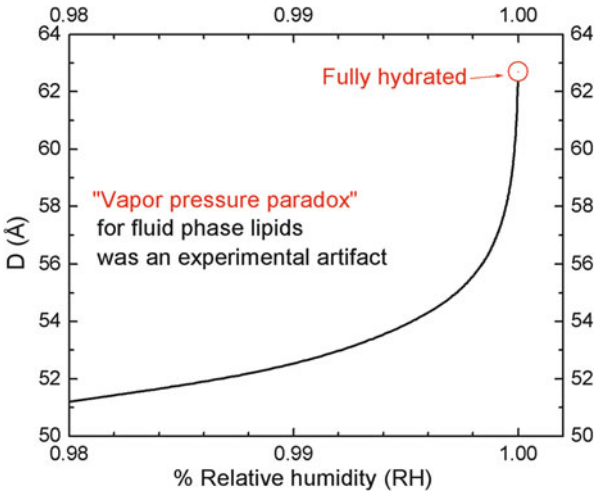

Fig. 2.11 Approximately 8 water molecules are taken up by DMPC in the final 0.2 % RH towards full hydration (Reproduced with permission from Fig. 3 (Chu et al. 2005))

not achieve the full n_W through the vapor (Jendrasiak and Hasty 1974; Torbet and Wilkins 1976). Our laboratory was successful in fully hydrating gel phase lipids through the vapor by placing the oriented sample on a Peltier cooling element within our X-ray hydration chamber, to gently condense all required water into the sample (Tristram-Nagle et al. 1993). Fluid phase lipid hydration through the vapor was much more difficult. See Fig. 2.11 for an example of the difficulty in attaining full hydration through the vapor.

This experimental hurdle was overcome with a well-insulated neutron hydration chamber (Katsaras 1998). Since that pioneering work, our laboratory has designed and built both a well-insulated X-ray (Kučerka et al. 2005a) and a well-insulated neutron chamber that each achieve full hydration of fluid phase lipids. The scattering from these samples is anisotropic similar to that shown in Fig. 2.6 for gel phase DMPC. K_C, the bending modulus, is an elastic parameter that characterizes the lipid membrane; it usually decreases when proteins are added (Tristram-Nagle and Nagle 2007; Shchelokovskyy et al. 2011; Pan et al. 2009a; Greenwood et al. 2008; Boscia

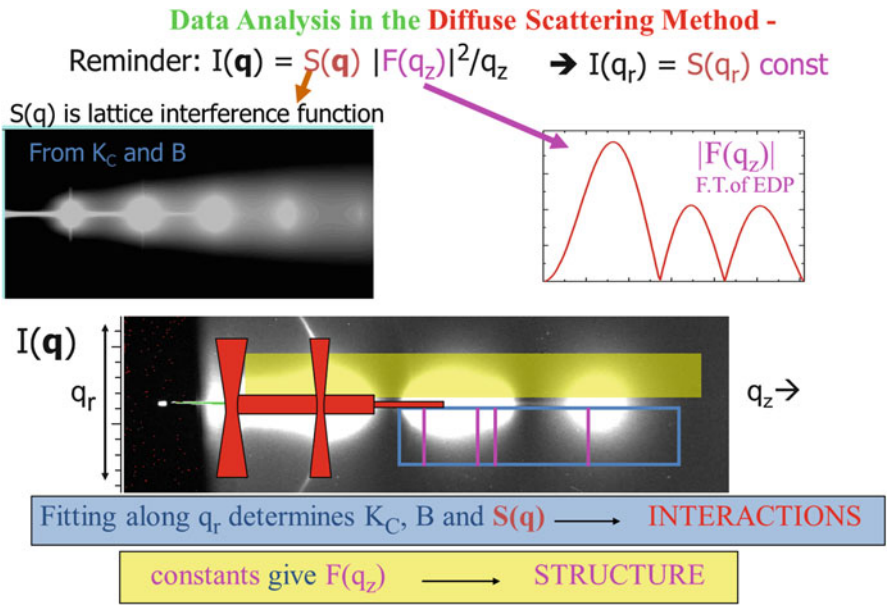

Fig. 2.12 Data analysis in the Diffuse Scattering Method first fits the X-ray diffuse data (*central image*) that results from fluctuating, fully hydrated bilayers in a stack to the liquid crystal theory using the free energy function shown in Fig. 2.9. This step obtains K_C, B and the structure factor shown in the *upper left*, by fitting the white intensity data in the diffuse lobes with 500 rays in q_r (some shown in magenta in the *grey box*). Then the q_z data under the yellow band are used to obtain the form factor by fixing the structure factor S(**q**). The intensity I(**q**) and the form factor $|(F(q_z)|$ are related by the equation shown at the top of this figure (Figure reproduced from Fig. 13 (Tristram-Nagle and Nagle 2004))

et al. 2013) and increases when cholesterol (Pan et al. 2008b, 2009b) or cardiolipin (Boscia et al. 2014) is added. A decrease in K_C indicates that it is easier to bend the membrane in the presence of a protein or peptide. K_C is determined *en route* to obtaining the structure factor, which then provides the form factor as is shown in Fig. 2.12.

Once the form factor is determined (brown curve in upper right of Fig. 2.12), the Scattering Density Profile (SDP) computer program is used to fit the form factor data to a model of a bilayer through the Fourier transform (Kučerka et al. 2008). The program models the component groups of a bilayer by using Gaussians for the two headgroup peaks, phosphocholine and glycerol-carbonyl, and for the methyl trough in the center of the bilayer, and by using error functions for the water and hydrocarbon electron densities. An example of an electron density profile determined by the SDP program is shown in Fig. 2.13 (solid lines). The profile also contains the bioflavinoid, BF, genistein. As shown, there is excellent agreement between the total and component electron densities when compared to the profile resulting from a CHARMM MD simulation carried out by Dr. Rich Pastor and Rick Venable at NHLBI (dotted lines).

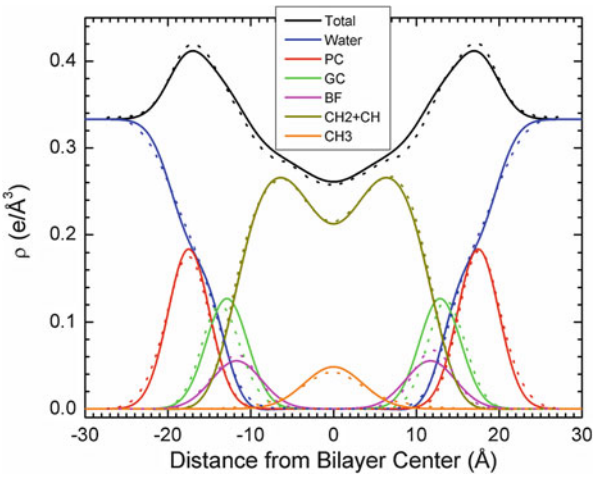

Fig. 2.13 Electron density profiles for DOPC with 20 mol % genistein resulting from SDP model fitting (*solid lines*) and MD simulations at $A_L = 83$ Å^2 (*dotted lines*). Component groups and bioflavinoid (BF) are identified in the legend (Reprinted (adapted) with permission from Fig. 4 (Raghunathan et al. 2012), American Chemical Society)

The SDP program also calculates bilayer thicknesses, $2D_C$ and D_B, as shown in the volume probabilities in Fig. 2.8c. Molecular volumes provide the underlying foundation upon which the SDP program is built; volume measurements will be discussed in Sect. 2.6. Using X-rays and, in some cases, X-rays plus neutrons, our laboratory has now determined many A_L's that have allowed the calculation of many n_W's using Eq. 2.1, shown in Table 2.1. n_W is 2–3 times larger in the fluid phase than in the gel phase, due to the larger A_L's and larger lamellar D-spacings (not shown). For fluid phase lipids, we rely more on the equilibrated D-spacings obtained by hydrating oriented samples through the vapor, than on the MLV capillary D-spacings. In many cases, the vapor-hydrated D-spacings are larger than the isotropic D-spacings, perhaps due to the artifact mentioned above caused by the constraining MLV geometry.

It is of interest to try to correlate A_L and n_W; this is done graphically in Fig. 2.14. As shown, n_W generally increases with A_L, both in the gel and fluid phases. The intuitive message is that larger lipid areas require more water. The increase is not linear, however, and is quite noisy since Eq. 2.1 involves other parameters besides A_L and n_W.

What about n_W', the steric number of water molecules associated with the headgroup molecule? For this, our group uses Eq. 2.6:

$$n_W' = \left(AD_H' - V_H\right)/V_W \tag{2.6}$$

where $A = A_L$, $D_H' = 9$ (PC's) or 8.5 (PE's) from neutron studies (Buldt et al. 1979), V_H = headgroup volume (Nagle and Tristram-Nagle 2000) and V_W is the volume of water. We can think of this water as headgroup structural water, shown in Fig. 2.7. It is considered to be a lower limit to measurements of tightly bound water. Using Eq. 2.6, n_W' is calculated for the lipids shown in Table 2.1. Values for n_W' are in the far right column in Table 2.1.

Again, n_W' is larger for fluid phase lipids than for gel phase lipids, but both are much smaller than n_W for their corresponding phase. n_W' shows a close correlation to A_L for fluid phase lipids when plotted in Fig. 2.15, with a nearly linear increase in n_W' between $A_L = 60–80$ Å^2. This indicates that a small number of water molecules (6–13) are closely associated with the fluid phase headgroup, part of its structure. For gel phase, n_W' is 3 for several lipids, except cardiolipin (TMCL) where it is 6 for this 4-chain lipid. DHPC in the interdigitated phase is not included in Fig. 2.15, since its bilayer thickness is much smaller than the other lipids. Remember that n_W' is merely calculated from our structural results; inclusion of headgroup n_W' results in a third measure of bilayer thickness, D_B', shown in Fig. 2.7c. Many investigators have attempted to measure tightly-coupled headgroup water using various experimental techniques. These results appear in Table 2.2 together with our calculated values of n_W' for DMPC and DPPC.

Interestingly, bound water, when measured by many different experimental techniques, shows little dependence on the lipid phase. Although some of the smallest n_W' (<5) are for gel phase DMPC and DPPC lipids, there is one small $n_W' = 4$ for fluid phase Egg PC. In addition, both gel phase and fluid phase lipids

Table 2.1 Lipid areas and associated water molecules (Nagle/Tristram-Nagle lab)

Lipid	T (°C)	Area ± 0.5 (Å^2)	n_W	n_W'
Fluid Phase				
DPPC	50	62.9(±1.3)[a], 64.0[b], 64.3[c], 63.1[d]*	30[a]	8[a]
DHPC	48	65.1[e]	33[e]	9[e]
DLPE	35	51.2[b]	9[b]	6[b]
DMPC	30	59.7[f], 60.6[g]	27[f]	7[f]
DLPC	30	63.2[g]	31[f]	8[f]
DOPC	30	72.2[h], 72.5[b], 72.1[i], 72.4[j, k], 67.4[d]*	33[h], 28[d]	11[h], 9[d]
	(15)	(69.1[k])	(30[k])	(10[k])
	(45)	(75.5[k])	(35[k])	(12[k])
DOPS	30	65.3[l]	∞[l]	10[l]
EggPC	30	69.4[f, b]	35[b]	10[b]
POPC	30	68.3(±1.5)[j]	31[j]	9[j]
SOPC	30	67.0(±0.9)[m]	30[m]	9[m]
diC22:1PC	30	69.3[j]	30[j]	10[j]
18:0–22:5PC	24	68.7[n]	30[n]	10[n]
18:0–22:6PC	24	68.2[n]	29[n]	9[n]
DiphytanoylPC	30	80.5(±1.5)[r]	37[r]	13[r]
DLPG	30	65.6[s]	∞[s]	9[s]
DMPG	30	65.1[s]	∞[s]	9[s]
POPG	30	66.1[s]	∞[s]	9[s]
SOPG	30	66.7[s]	∞[s]	9[t]
DOPG	30	70.8[s]	∞[s]	10[s]
TMCL	50	108.6[t]	∞[t]	14[t]

(continued)

Table 2.1 (continued)

Lipid	T (°C)	Area ± 0.5 (Å^2)	n_W	n_W'
Gel Phase				
DMPC	10	47.2[o]	12°	3°
DiC16PC,18,20,22,24	20	47.5[p, q]	12[p]	3[p]
DMPS	20	40.8[l]	∞[l]	3[l]
DLPE	20	41.0[b]	6[b]	3[b]
DHPC-Interdig	20	77.2[e]	24[e]	12[e]
DHPC-gel	20	46.9[e]	10[e]	3[e]
TMCL	35	81.5[t]	∞[t]	6[t]

[a]Nagle et al. (1996)
[b]Nagle and Tristram-Nagle (2000)
[c]Kučerka et al. (2006)
[d]Kučerka et al. (2008)
[e]Guler et al. (2009)
[f]Petrache et al. (1998b)
[g]Kučerka et al. (2005a)
[h]Tristram-Nagle et al. (1998)
[i]Liu and Nagle (2004)
[j]Kučerka et al. (2005b)
[k]Pan et al. (2008a)
[l]Petrache et al. (2004)
[m]Greenwood et al. (2008)
[n]Eldho et al. (2003)
[o]Tristram-Nagle et al. (2002)
[p]Tristram-Nagle et al. (1993)
[q]Sun et al. (1996)
[r]Tristram-Nagle et al. (2010)
[s]Pan et al. (2012)
[t]Boscia et al. (2014)
*Neutron data

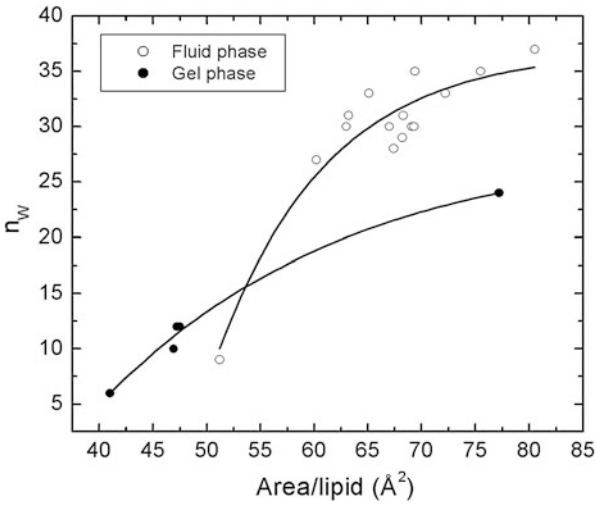

Fig. 2.14 Number of water molecules/lipid, n_W, vs. area/lipid, A_L

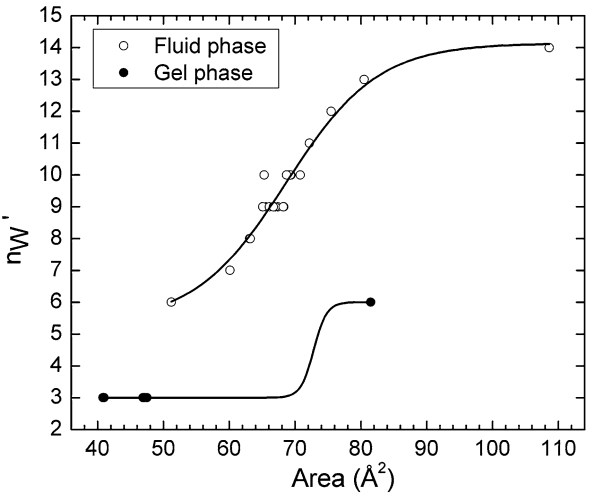

Fig. 2.15 Number of water molecules/lipid, n_W', vs. area/lipid, A_L

Table 2.2 Bound water, $n_{W'}$, determined experimentally

Authors (year)	Method	$n_{W'}$
Bach and Miller (1998)	Unfreezable water DSC (DMPC)	3.5
Salsbury et al. (1972) (& Chapman)	^{2}NMR linewidths in inner hydration shell (Egg PC)	4
Miller et al. (2002) (& Kodama)	Unfreezable water DSC (DMPC)	4.5
Bronshteyn and Steponkus (1993)	Unfreezable water DSC (DPPC)	5
Jendrasiak and Hasty (1974)	Inflection point in adsorption isotherm (DPPC)	5
Channareddy et al. (1997) (& Janes)	Radiolabel, sucrose & centrifugation (EggPC)	7
Binder et al. (1999) (& Heerklotz)	Isothermal titration calorimetry, gravimetry & FTIR (POPC)	~7
Pohle et al. (1998)	Adsorption isotherm using FTIR (DPPC)	7
Crowe et al. (1994)	Unfreezable water DSC (DPPC)	7.2
Nagle and Tristram-Nagle (2000)	X-ray fluid phase area, V_L, calculations (DMPC (30 °C) and DPPC (50 °C))	7, 8
Small (1967)	X-ray gravimetric, volumetric considerations (Egg PC)	8.3
Salsbury et al. (1972) (& Chapman)	^{2}NMR linewidths in inner hydration shell (gel phase DPPC)	9
Dufourcq et al. (1997)	Solid state NMR hydration regime (fluid phase DMPC)	9.7
Grdadolnik and Hadzi (1994)	FTIR bandshape and unfreezable water (DPPC)	10
Finer and Darke (1974)	^{2}NMR linewidths in inner hydration shell (Egg PC)	11
Hristova and White (1998)	Change in lipid structure using X-ray electron density profiles (DOPC)	12
Lairion et al. (2002) (& Disalvo)	Reverse micelles & turbidity (Egg PC)	12

have comparable values when $n_W' = 7$ or greater. Our lab's calculated steric values of 7 and 8 for fluid phase DMPC and DPPC, respectively, are near the middle of this range of experimental values. Some of the smallest values are for unfreezable water in DSC where the lipid is presumably in the gel phase, but one value is 7.2 (Crowe et al. 1994). Depending on the cooling rate, the lipid could be in the subgel phase, which requires less water than the gel phase. If the cooling rate is very slow, ice crystals can form in pools of water which create an osmotic pressure, lowering headgroup water. Unlike the gravimetric method, unfreezable water does not have to be sandwiched between bilayers, but simply associated with the phospholipid headgroup. In many of these studies, not only was an inner hydration shell found (reported in Table 2.2), but 1 or 2 outer hydration shells were found, before bulk water partitioned out. While these other hydration shells are of some interest, it has been shown using ^{2}H-NMR that hydration of DOPC is a smooth, continuous process, without separate hydration shells (Ulrich and Watts 1994). In that study, n_W' for DOPC = 22. The main point in showing values of headgroup water in Table 2.2 is to emphasize the large range of experimental values that have been reported in the literature. Perhaps it is not accurate to list these values in the same table, because they may be measuring different quantities.

2.6 Obtaining Molecular Volumes

As mentioned above, molecular volumes, V_L, are needed to calculate n_W and also to determine structure using the SDP modeling program. When I first joined the Nagle laboratory as a postdoc in 1982, I worked with a home-built instrument, the differential scanning dilatometer (DSD). It was constructed by John Nagle and his former postdoc Allan Wilkinson and was necessarily housed in the basement of Mellon Institute, to minimize vibrations. A grainy image of this instrument is shown in Fig. 2.16. The principle of the dilatometer is that expansion of a large volume of 0.2–1 g lipid in 10 ml water is compared to the expansion of 10 ml water as the temperature is increased. The lipid was in the form of MLVs, described in Sect. 2.2. The instrument was time-consuming to operate, since the glass stopcocks on top of the fragile glass "arms" had to be manually opened and closed often to release the pressure buildup after a few temperature increments, every 5 min. The 3D volume change in the lipid and water was transduced to a 2D vertical movement of the metal bellows shown in Fig. 2.16b. These bellows caused a precise movement of an optical flat; this movement was recorded using a laser that produced an interference pattern between the moving optical flat and a stationary optical flat below it (piezo-interferometry). The # fringes in the interference pattern were recorded manually by the operator, and a complete description of this instrument was published (Wilkinson and Nagle 1978). Although the dilatometer was difficult to operate, it was used to obtain many precise lipid volume measurements (Tristram-Nagle et al. 1987; Wiener et al. 1988; Wilkinson and McIntosh 1986; Wilkinson and

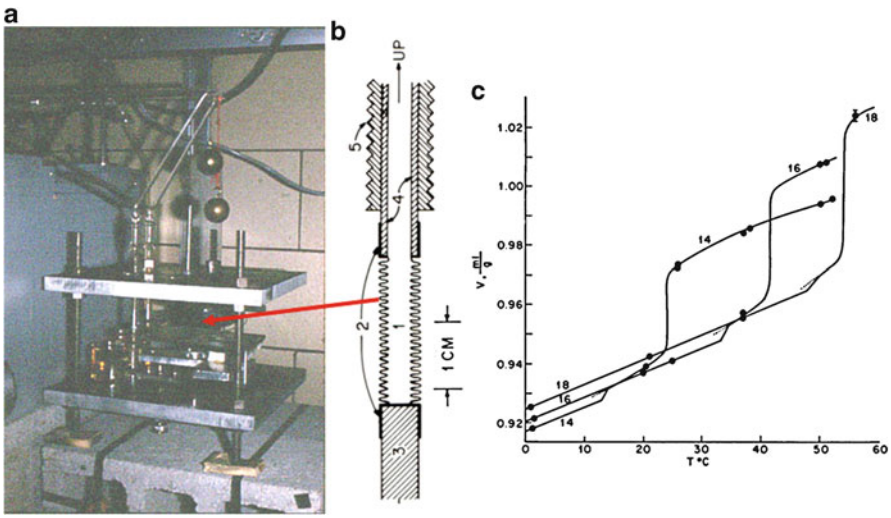

Fig. 2.16 (**a**) Differential scanning dilatometer with sample flasks extending into the grey water bath at *left of picture*. (**b**) Schematic of bellows containing a heavy hydrocarbon fluid in contact with expanding water. *Red arrow* shows their location in the dilatometer. (**c**) Specific volume data obtained using the dilatometer (*solid lines*) pinned to values obtained using neutral flotation (*solid circles*) (Data for DMPC (14), DPPC (16) and DSPC (18) reproduced with permission from Fig. 1 (Nagle and Wilkinson 1978))

Nagle 1979, 1981, 1984; Wilkinson et al. 1987; Yang and Nagle 1988). The DSD was also useful in obtaining α, the coefficient of thermal expansion. The change in volume vs. temperature reveals information regarding intermolecular interactions in the single phase regions (Wilkinson and Nagle 1982; Tristram-Nagle et al. 1986), as well as the total volume change during phase transitions (Nagle and Wilkinson 1978).

Besides its inconvenience, the differential dilatometer could only obtain relative, not absolute volumes. For this, the Nagle/Tristram-Nagle lab used neutral flotation (or neutral buoyancy) of lipids in D_2O/H_2O mixtures. The validity of neutral flotation for lipid bilayer dispersions was tested in (Wiener et al. 1988). The principle of this method is to prepare several D_2O/H_2O mixtures with specific densities (g/ml) (inverse specific volume) near to the expected lipid specific density. Volumes (1/densities) are first estimated by comparing to other lipids or by calculating the total volume using the component group volumes. An example of several mixtures prepared to measure the volume of DPPC at 21 °C is shown in Fig. 2.17a. The lipid will sink, swim or float as shown in Fig. 2.17b. Centrifugation can accelerate this process, but 2 days equilibrating in a temperature-controlled Incufridge is sufficient to produce the result shown in Fig. 2.17a. As shown, DPPC at 21 °C swims (is neutrally buoyant) at a density of 1.0705 g/ml. Density is converted to molecular volume using Eq. 2.7, where GMW is the gram molecular weight.

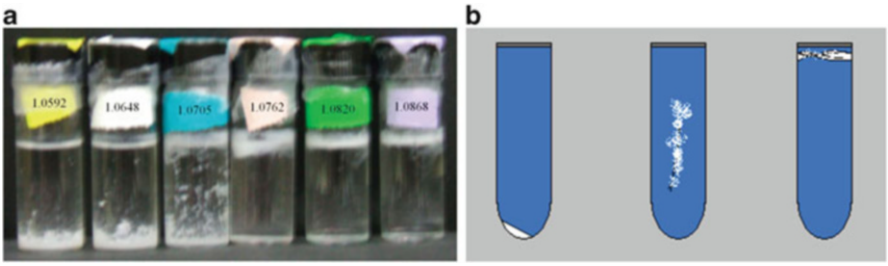

Fig. 2.17 (**a**) D_2O/H_2O solutions prepared with the densities shown contain DPPC (Reproduced with permission from Fig. 1 (Hallinen et al. 2012) from the PCCP Owner Societies). (**b**) Diagram showing three different lipid positions in a tube containing known densities

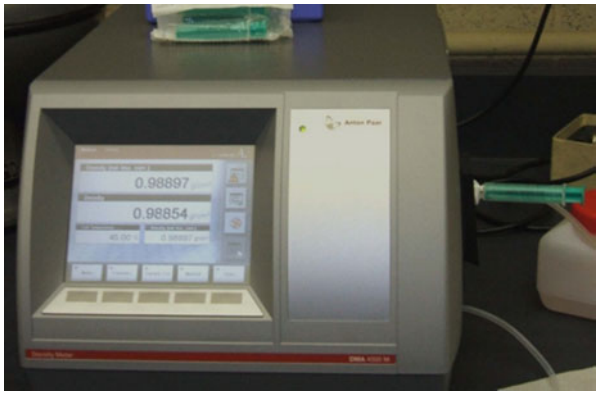

Fig. 2.18 Anton-Paar 5000M vibrating tube densimeter with sample syringe

$$Density\ (\mathrm{g/ml})\, x \left(\frac{1\ \text{mole}}{GMW}\right) x \left(\frac{6.022 \times 10^{23}\ \text{molecules}}{1\ \text{mole}}\right) x \left(\frac{1\ \text{ml}}{10^{24}\text{Å}^3}\right) = \left(\frac{1}{V_L\text{Å}^3}\right) \tag{2.7}$$

The third method that our lab currently uses to obtain volumes is with a modern Anton-Paar DMA 5000 M densimeter. A picture of this instrument is shown in Fig. 2.18.

The operating principle of the densimeter is that the frequency of oscillation of a vibrating tube will be damped, i.e., the period τ will increase, when the solvent density ρ_S increases. Since it is a differential instrument, ρ_0, which is the density of a vibrating tube filled with air, is subtracted from ρ_S as shown in Eq. 2.8. K is an instrumental constant that depends on the barometric pressure in the laboratory.

$$\rho_S - \rho_0 = K\left(\tau_S^2 - \tau_0^2\right) \tag{2.8}$$

Normally fairly dilute MLV suspensions of lipids or lipid/protein mixtures are prepared (2–5 wt%). It is important that the concentration is known precisely since

the density from this dilute solution is extrapolated to 100 % lipid or lipid/protein mixture. Generally 50 mg lipid in 1.2 ml MilliQ water is used for the densimeter experiment. The molecular volume is calculated using Eq. 2.9, where ρ_W is the density of water at a specific temperature, m_W = mass of water, m_L = mass of lipid or lipid/mixture and M_L = GMW.

$$V_L = \frac{M_L}{0.6022 P_S}\left[1 + \frac{m_W}{m_L}\left(1 - \frac{\rho_S}{\rho_W}\right)\right] \tag{2.9}$$

For lipids that have been measured by both neutral flotation and densimetry, we have obtained quite good agreement provided that the densimeter sample is at least 5 wt% and that it is bubble-free. The samples are not degassed to avoid changes in concentration; however, they usually stand for one day prior to measurement to reduce bubble formation. For this same reason, measurements in the densimeter are confined to <50 °C. The densimeter is housed in a clear plastic box to reduce air drafts. We did encounter an artifact using the densimeter whereupon repeatedly scanning a lipid suspension up and down in temperature, the density appeared to increase. When we remixed the sample by removing and replacing it in the densimeter, the density returned to its original value (Hallinen et al. 2012). If care is taken with the sample preparation and loading procedure, then the Anton-Paar 5000 M densimeter obtains molecular volumes quite close to those obtained by neutral flotation. An example of this good agreement is shown in Fig. 2.19. The diphytanoylPC volume obtained using densimetry was 1425 Å^3 while that obtained using neutral buoyancy was 1435 Å^3.

As described above in Sect. 2.4, the headgroup volume V_H, is needed to determine A_L for X-ray data using Eq. 2.3. How do we know V_H? For PC lipids, we determined V_H by fitting well-determined DMPC gel phase data with a model of a bilayer (Tristram-Nagle et al. 2002). In that work, A_L was determined both using oriented WAXS as described in Sect. 2.3, and also by fitting 10 lamellar orders of

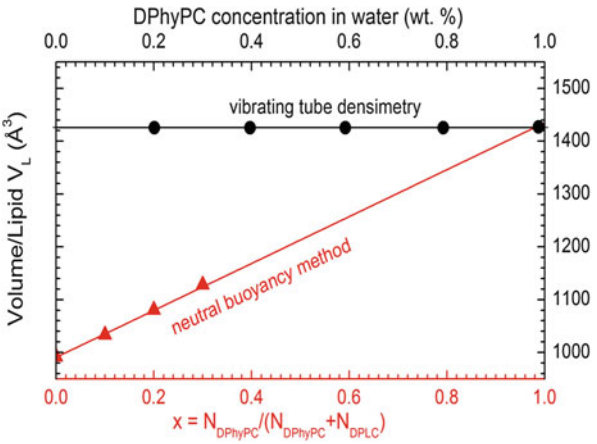

Fig. 2.19 Molecular volume of diphytanoylPC obtained using vibrating tube densimetry (*black circles*) compared to neutral buoyancy (*red triangles*) (Reproduced with permission from Fig. 2 (Tristram-Nagle et al. 2010))

LAXS. This study yielded 331 $Å^3$ for the PC headgroup which was close to an earlier value obtained by our lab of 319 $Å^3$ (Sun et al. 1994). We assume that V_H does not change with temperature because when the chain melting transitions (Tms) of lipids with n carbons/chain were plotted vs. 1(/n−3), a linear fit extrapolated to the melting temperature of polyethylene, indicating that the headgroup does not "melt" with increasing temperature (Nagle and Wilkinson 1978). For the PE lipids, we relied on the X-ray gel electron density profiles of McIntosh (Mcintosh and Simon 1986) and our own volumetric measurements (Wiener et al. 1988) to determine $V_H = 252$ $Å^3$. For PS lipids, we similarly used gel phase X-ray electron density profiles to determine that $V_H = 244$ $Å^3$ (Petrache et al. 2004). For PG lipids, we joined forces with Pan's team to determine that the headgroup volume is 291 $Å^3$, this time using X-ray and neutron scattering data to obtain precise structural parameters. Recently we determined that for ½ TMCL (4-chain cardiolipin), $V_H = 253$ $Å^3$, close to that of PE lipids.

To conclude, this chapter summarizes early membrane models and experiments to characterize the structure and thermodynamic properties of hydrated lipid bilayers. It discusses the problems with the gravimetric method to determine n_W. It describes in detail how the Nagle/Tristram-Nagle laboratory use LAXS and WAXS, and neutron scattering, to precisely determine A_L, which is then used to calculate n_W, the total number of water molecules/lipid, and n_W', the steric water near the lipid headgroup. Details of experiments to determine the volume, which is the foundation of the X-ray structural work, are also presented. Finally, a summary of many literature experiments to determine constrained headgroup water is presented in Table 2.2.

Acknowledgements The author would like to thank Ben Sauerwine for preparing the snapshot of fluctuating bilayers from the Monte Carlo simulation. Funding was from NIH GM 44976.

References

Bach D, Miller IR (1998) Hydration of phospholipid bilayers in the presence and absence of cholesterol. Biochim Biophys Acta 1368(2):216–224

Binder H, Kohlstrunk B, Heerklotz HH (1999) Hydration and lyotropic melting of amphiphilic molecules: a thermodynamic study using humidity titration calorimetry. J Colloid Interface Sci 220(2):235–249

Boscia AL, Akabori K, Benamram Z, Michel JA, Jablin MS, Steckbeck JD, Montelaro RC, Nagle JF, Tristram-Nagle S (2013) Membrane structure correlates to function of LLP2 on the cytoplasmic tail of HIV-1 gp41 protein. Biophys J 105(3):657–666

Boscia AL, Treece BW, Mohammadyani D, Klein-Seetharaman J, Braun AR, Wassenaar TA, Klosgen B, Tristram-Nagle S (2014) X-ray structure, thermodynamics, elastic properties and MD simulations of cardiolipin/dimyristoylphosphatidylcholine mixed membranes. Chem Phys Lipids 178:1–10

Bronshteyn VL, Steponkus PL (1993) Calorimetric studies of freeze-induced dehydration of phospholipids. Biophys J 65(5):1853–1865

Buldt G, Gally HU, Seelig J, Zaccai G (1979) Neutron-diffraction studies on phosphatidylcholine model membranes. 1. Head group conformation. J Mol Biol 134(4):673–691
Caillé A (1972) X-ray scattering by smectic-A crystals. CR Acad Sci Paris Sér B 274:891–893
Channareddy S, Jose SS, Janes N (1997) Direct determination of hydration in the lamellar to inverted hexagonal transition of phosphatidylethanolamine. J Am Chem Soc 119:2345–2347
Chu N, Kučerka N, Liu YF, Tristram-Nagle S, Nagle JF (2005) Anomalous swelling of lipid bilayer stacks is caused by softening of the bending modulus. Phys Rev E 71(4):041904
Crowe LM, Spargo BJ, Ioneda T, Beaman BL, Crowe JH (1994) Interaction of cord factor (alpha, alpha′-trehalose-6,6′-dimycolate) with phospholipids. Biochim Biophys Acta Biomembr 1194:53–60
Danielli JF, Davson H (1935) A contribution to the theory of permeability of thin films. J Cell Comp Physiol 5(4):495–508
de Gennes PG, Prost J (1993) The physics of liquid crystals, 2nd edn. Oxford University Press, New York
Dufourcq P, Louis H, Dandre F, Lavie J, Bonnet J, Lamaziere JM (1997) Phenotypic modification of arterial smooth muscle cells in response to medial dissection. Coron Artery Dis 8(3–4):163–170
Eldho NV, Feller SE, Tristram-Nagle S, Polozov IV, Gawrisch K (2003) Polyunsaturated docosahexaenoic vs docosapentaenoic acid – differences in lipid matrix properties from the loss of one double bond. J Am Chem Soc 125(21):6409–6421
Finer EG, Darke A (1974) Phospholipid hydration studied by deuteron magnetic resonance spectroscopy. Chem Phys Lipids 12(1):1–16
Frye LD, Edidin M (1970) The rapid intermixing of cell surface antigens after formation of mouse-human heterokaryons. J Cell Sci 7(2):319–335
Gallova J, Uhrikova D, Kučerka N, Teixeira J, Balgavy P (2008) Hydrophobic thickness, lipid surface area and polar region hydration in monounsaturated diacylphosphatidylcholine bilayers: SANS study of effects of cholesterol and beta-sitosterol in unilamellar vesicles. Biochim Biophys Acta 1778(11):2627–2632
Gawrisch K, Richter W, Mops A, Balgavy P, Arnold K, Klose G (1985) The influence of water concentration on the structure of egg-yolk phospholipid water dispersions. Stud Biophys 108(1):5–16
Gorter E, Grendel F (1925) On bimolecular layers of lipoids on the chromocytes of the blood. J Exp Med 41(4):439–443
Gouliaev N, Nagle JF (1998) Simulations of interacting membranes in the soft confinement regime. Phys Rev Lett 81(12):2610–2613
Grdadolnik J, Hadzi D (1994) Conformational effects of metal salt binding to the polar head of phosphatidylcholines investigated by FTIR spectroscopy. Chem Phys Lipids 65:121–132
Greenwood AI, Pan JJ, Mills TT, Nagle JF, Epand RM, Tristram-Nagle S (2008) CRAC motif peptide of the HIV-1 gp41 protein thins SOPC membranes and interacts with cholesterol. Biochim Biophys Acta Biomembr 1778(4):1120–1130
Guinier A (1963) X-ray diffraction in crystals, imperfect crystals, and amorphous bodies. W. H. Freeman, San Francisco
Guler SD, Ghosh DD, Pan JJ, Mathai JC, Zeidel ML, Nagle JF, Tristram-Nagle S (2009) Effects of ether vs. ester linkage on lipid bilayer structure and water permeability. Chem Phys Lipids 160(1):33–44
Hallinen KM, Tristram-Nagle S, Nagle JF (2012) Volumetric stability of lipid bilayers. Phys Chem Chem Phys 14(44):15452–15457
Hosemann R, Bagchi SN (1962) Direct analysis of diffraction by matter. North-Holland, Amsterdam
Hristova K, White SH (1998) Determination of the hydrocarbon core structure of fluid dioleoylphosphocholine (DOPC) bilayers by x-ray diffraction using specific bromination of the double-bonds: effect of hydration. Biophys J 74(5):2419–2433
Jendrasiak GL, Hasty JH (1974) The hydration of phospholipids. Biochim Biophys Acta 337(1):79–91

Katsaras J (1998) Adsorbed to a rigid substrate, dimyristoylphosphatidylcholine multibilayers attain full hydration in all mesophases. Biophys J 75(5):2157–2162

Klose G, Konig B, Meyer HW, Schulze G, Degovics G (1988) Small-angle X-ray-scattering and electron-microscopy of crude dispersions of swelling lipids and the influence of the morphology on the repeat distance. Chem Phys Lipids 47(3):225–234

Koenig BW, Strey HH, Gawrisch K (1997) Membrane lateral compressibility determined by NMR and X-ray diffraction: effect of acyl chain polyunsaturation. Biophys J 73(4):1954–1966

Kučerka N, Kiselev MA, Balgavy P (2004) Determination of bilayer thickness and lipid surface area in unilamellar dimyristoylphosphatidylcholine vesicles from small-angle neutron scattering curves: a comparison of evaluation methods. Eur Biophys J Biophys 33(4):328–334

Kučerka N, Liu YF, Chu NJ, Petrache HI, Tristram-Nagle ST, Nagle JF (2005a) Structure of fully hydrated fluid phase DMPC and DLPC lipid bilayers using X-ray scattering from oriented multilamellar arrays and from unilamellar vesicles. Biophys J 88(4):2626–2637

Kučerka N, Tristram-Nagle S, Nagle JF (2005b) Structure of fully hydrated fluid phase lipid bilayers with monounsaturated chains. J Membr Biol 208(3):193–202

Kučerka N, Tristram-Nagle S, Nagle JF (2006) Closer look at structure of fully hydrated fluid phase DPPC bilayers. Biophys J 90(11):L83–L85

Kučerka N, Nagle JF, Sachs JN, Feller SE, Pencer J, Jackson A, Katsaras J (2008) Lipid bilayer structure determined by the simultaneous analysis of neutron and x-ray scattering data. Biophys J 95(5):2356–2367

Ladbrook BD, Williams RM, Chapman D (1968) Studies on lecithin-cholesterol-water interactions by differential scanning calorimetry and X-ray diffraction. Biochim Biophys Acta 150(3):333–340

Lairion F, Filler R, Disalvo EA (2002) Reversed micelles as model systems to study interfacial properties of lipid bilayers. Colloid Surf B 25(4):369–371

Levine YK (1973) X-ray diffraction studies of membranes. Prog Surf Sci 3:279–352

Lewis BA, Engelman DM (1983) Lipid bilayer thickness varies linearly with acyl chain-length in fluid phosphatidylcholine vesicles. J Mol Biol 166(2):211–217

Liu YF, Nagle JF (2004) Diffuse scattering provides material parameters and electron density profiles of biomembranes. Phys Rev E 69(4):040901

Lyatskaya Y, Liu YF, Tristram-Nagle S, Katsaras J, Nagle JF (2001) Method for obtaining structure and interactions from oriented lipid bilayers. Phys Rev E 63(1):011907

Mcintosh TJ, Simon SA (1986) Area per molecule and distribution of water in fully hydrated dilauroylphosphatidylethanolamine bilayers. Biochemistry 25(17):4948–4952

Mendelsohn R, Davies MA, Schuster HF, Xu ZC, Bittman R (1991) Cd2 rocking modes as quantitative infrared probes of one-bond, 2-bond, and 3-bond conformational disorder in dipalmitoylphosphatidylcholine and dipalmitoylphosphatidylcholine cholesterol mixtures. Biochemistry 30(35):8558–8563

Miller IR, Bach D, Wachtel EJ, Eisenstein M (2002) Interrelation between hydration and interheadgroup interaction in phospholipids. Bioelectrochemistry 58(2):193–196

Mills TT, Toombes GES, Tristram-Nagle S, Smilgies DM, Feigenson GW, Nagle JF (2008) Order parameters and areas in fluid-phase oriented lipid membranes using wide angle x-ray scattering. Biophys J 95(2):669–681

Nagle JF (1976) Theory of lipid monolayer and bilayer phase-transitions – effect of headgroup interactions. J Membr Biol 27(3):233–250

Nagle JF (1980) Theory of the main lipid bilayer phase transition. Annu Rev Phys Chem 31:157–195

Nagle JF, Tristram-Nagle S (2000) Structure of lipid bilayers. Biochim Biophys Acta Rev Biomembr 1469(3):159–195

Nagle JF, Wilkinson DA (1978) Lecithin bilayers – density measurements and molecular interactions. Biophys J 23(2):159–175

Nagle JF, Zhang RT, Tristram-Nagle S, Sun WJ, Petrache H, Suter RM (1996) X-ray structure determination of fully hydrated L(alpha) phase DPPC bilayers. Biophys J 70(2):1419–1431

Pan J, Tristram-Nagle S, Kučerka N, Nagle JF (2008a) Temperature dependence of structure, bending rigidity, and bilayer interactions of dioleoylphosphatidylcholine bilayers. Biophys J 94(1):117–124

Pan JJ, Mills TT, Tristram-Nagle S, Nagle JF (2008b) Cholesterol perturbs lipid bilayers nonuniversally. Phys Rev Lett 100(19)

Pan JJ, Tieleman DP, Nagle JF, Kučerka N, Tristram-Nagle S (2009a) Alamethicin in lipid bilayers: combined use of X-ray scattering and MD simulations. Biochim Biophys Acta Biomembr 1788(6):1387–1397

Pan JJ, Tristram-Nagle S, Nagle JF (2009b) Effect of cholesterol on structural and mechanical properties of membranes depends on lipid chain saturation. Phys Rev E 80(2):021931

Pan JJ, Heberle FA, Tristram-Nagle S, Szymanski M, Koepfinger M, Katsaras J, Kučerka N (2012) Molecular structures of fluid phase phosphatidylglycerol bilayers as determined by small angle neutron and X-ray scattering. Biochim Biophys Acta Biomembr 1818(9):2135–2148

Petrache HI, Gouliaev N, Tristram-Nagle S, Zhang RT, Suter RM, Nagle JF (1998a) Interbilayer interactions from high-resolution x-ray scattering. Phys Rev E 57(6):7014–7024

Petrache HI, Tristram-Nagle S, Nagle JF (1998b) Fluid phase structure of EPC and DMPC bilayers. Chem Phys Lipids 95(1):83–94

Petrache HI, Tristram-Nagle S, Gawrisch K, Harries D, Parsegian VA, Nagle JF (2004) Structure and fluctuations of charged phosphatidylserine bilayers in the absence of salt. Biophys J 86(3):1574–1586

Pohle W, Selle C, Fritzsche H, Binder H (1998) Fourier transform infrared spectroscopy as a probe for the study of the hydration of lipid self-assemblies. I. Methodology and general phenomena. Biospectroscopy 4(4):267–280

Raghunathan M, Zubovski Y, Venable RM, Pastor RW, Nagle JF, Tristram-Nagle S (2012) Structure and elasticity of lipid membranes with genistein and daidzein bioflavinoids using X-ray scattering and MD simulations. J Phys Chem B 116(13):3918–3927

Rand RP, Parsegian VA (1989) Hydration forces between phospholipid bilayers. Biochim Biophys Acta 988(3):351–376

Robertson JD (1960) The molecular structure and contact relationships of cell membranes. Prog Biophys Mol Biol 10:343–418

Salsbury NJ, Chapman D, Darke A (1972) Deuteron magnetic-resonance studies of water associated with phospholipids. Chem Phys Lipids 8(2):142–151

Shchelokovskyy P, Tristram-Nagle S, Dimova R (2011) Effect of the HIV-1 fusion peptide on the mechanical properties and leaflet coupling of lipid bilayers. New J Phys 13:025004

Simons K, Toomre D (2000) Lipid rafts and signal transduction. Nat Rev Mol Cell Biol 1(1):31–39

Singer SJ, Nicolson GL (1972) The fluid mosaic model of the structure of cell membranes. Science 175(4023):720–731

Small DM (1967) Phase equilibria and structure of dry and hydrated egg lecithin. J Lipid Res 8(6):551–557

Sun W, Suter RM, Knewtson MA, Worthington CR, Tristram-Nagle S, Zhang R, Nagle JF (1994) Order and disorder in fully hydrated unoriented bilayers of gel-phase dipalmitoylphosphatidylcholine. Phys Rev E Stat Phys Plasmas Fluids Relat Interdiscip Topics 49(5):4665–4676

Sun WJ, Tristram-Nagle S, Suter RM, Nagle JF (1996) Structure of gel phase saturated lecithin bilayers: temperature and chain length dependence. Biophys J 71(2):885–891

Swart SP (1907) About the permeability of artificial lipid membranes for proferments. Biochem Z 6:358–365

Tardieu A, Luzzati V, Reman FC (1973) Structure and polymorphism of the hydrocarbon chains of lipids: a study of lecithin-water phases. J Mol Biol 75(4):711–733

Torbet J, Wilkins MHF (1976) X-Ray diffraction studies of lecithin bilayers. J Theor Biol 62(2):447–458

Tristram-Nagle SA (2007) Preparation of oriented, fully hydrated lipid samples for structure determination using X-ray scattering. Methods Mol Biol 400:63–75

Tristram-Nagle S, Nagle JF (2004) Lipid bilayers: thermodynamics, structure, fluctuations, and interactions. Chem Phys Lipids 127(1):3–14

Tristram-Nagle S, Nagle JF (2007) HIV-1 fusion peptide decreases bending energy and promotes curved fusion intermediates. Biophys J 93(6):2048–2055
Tristram-Nagle S, Yang CP, Nagle JF (1986) Thermodynamic studies of purple membrane. Biochim Biophys Acta 854(1):58–66
Tristram-Nagle S, Wiener MC, Yang CP, Nagle JF (1987) Kinetics of the subtransition in dipalmitoylphosphatidylcholine. Biochemistry Us 26(14):4288–4294
Tristram-Nagle S, Zhang R, Suter RM, Worthington CR, Sun WJ, Nagle JF (1993) Measurement of chain tilt angle in fully hydrated bilayers of gel phase lecithins. Biophys J 64(4):1097–1109
Tristram-Nagle S, Petrache HI, Nagle JF (1998) Structure and interactions of fully hydrated dioleoylphosphatidylcholine bilayers. Biophys J 75(2):917–925
Tristram-Nagle S, Liu YF, Legleiter J, Nagle JF (2002) Structure of gel phase DMPC determined by X-ray diffraction. Biophys J 83(6):3324–3335
Tristram-Nagle S, Kim DJ, Akhunzada N, Kučerka N, Mathai JC, Katsaras J, Zeidel M, Nagle JF (2010) Structure and water permeability of fully hydrated diphytanoylPC. Chem Phys Lipids 163(6):630–637
Ulrich AS, Watts A (1994) Molecular response of the lipid headgroup to bilayer hydration monitored by H2-Nmr. Biophys J 66(5):1441–1449
Wiener MC, Tristram-Nagle S, Wilkinson DA, Campbell LE, Nagle JF (1988) Specific volumes of lipids in fully hydrated bilayer dispersions. Biochim Biophys Acta 938(2):135–142
Wilkinson DA, McIntosh TJ (1986) A subtransition in a phospholipid with a net charge, dipalmitoylphosphatidylglycerol. Biochemistry 25(2):295–298
Wilkinson DA, Nagle JF (1978) Differential dilatometer. Anal Biochem 84(1):263–271
Wilkinson DA, Nagle JF (1979) Dilatometric study of binary mixtures of phosphatidylcholines. Biochemistry 18(19):4244–4249
Wilkinson DA, Nagle JF (1981) Dilatometry and calorimetry of saturated phosphatidylethanolamine dispersions. Biochemistry 20(1):187–192
Wilkinson DA, Nagle JF (1982) Specific heats of lipid dispersions in single-phase regions. Biochim Biophys Acta 688(1):107–115
Wilkinson DA, Nagle JF (1984) Metastability in the phase behavior of dimyristoylphosphatidylethanolamine bilayers. Biochemistry 23(7):1538–1541
Wilkinson DA, Tirrell DA, Turek AB, McIntosh TJ (1987) Tris buffer causes acyl chain interdigitation in phosphatidylglycerol. Biochim Biophys Acta 905(2):447–453
Yang CP, Nagle JF (1988) Phase transformations in lipids follow classical kinetics with small fractional dimensionalities. Phys Rev A 37(10):3993–4000
Zhang R, Suter RM, Nagle JF (1994) Theory of the structure factor of lipid bilayers. Phys Rev E Stat Phys Plasmas Fluids Relat Interdiscip Topics 50(6):5047–5060
Zhang R, Sun WJ, Tristram-Nagle S, Headrick RL, Suter RM, Nagle JF (1995) Critical fluctuations in membranes. Phys Rev Lett 74(14):2832–2835
Zhang R, Tristram-Nagle S, Sun WJ, Headrick RL, Irving TC, Suter RM, Nagle JF (1996) Small-angle X-ray scattering from lipid bilayers is well described by modified Caillé theory but not by paracrystalline theory. Biophys J 70(1):349–357